Spatiotemporal Fuzzy-Observer-based Feedback Control for Networked Parabolic PDE Systems

Jun-Wei Wang, Yun Feng, Stevan Dubljevic, and Hak-Keung Lam

***Abstract*—Assisted by the Takagi-Sugeno (T-S) fuzzy model-based nonlinear control technique, nonlinear spatiotemporal feedback compensators are proposed in this article for exponential stabilization of parabolic partial differential dynamic systems with measurement outputs transmitted over a communication network. More specifically, an approximate T-S fuzzy partial differential equation (PDE) model with C^{∞}-smooth membership functions is constructed to describe the complex spatiotemporal dynamics of the nonlinear partial differential systems, and its approximation capability is analyzed via the uniform approximation theorem on a real separable Hilbert space. A spatiotemporally asynchronous sampled-data measurement output equation is proposed to model the transmission process of networked measurement outputs. By the approximate T-S fuzzy PDE model, fuzzy-observer-based nonlinear continuous-time and sampled-data feedback compensators are constructed via the spatiotemporally asynchronous sampled-data measurement outputs. Given that sufficient conditions presented in terms of linear matrix inequalities are satisfied, the suggested fuzzy compensators can exponentially stabilize the nonlinear system in the Lyapunov sense. Simulation results are presented to show the effectiveness and merit of the suggested spatiotemporal fuzzy compensators.**

***Index Terms*—Networked control systems, sampled-data systems, exponential stabilization, partial differential equation, spatiotemporal Takagi-Sugeno fuzzy model.**

I. Introduction

A. Research Background

NETWORKED CONTROL SYSTEMS (NCSs) are a class of cyber-physical systems where the cyber-layer (e.g., controller) is interconnected with the physical system through some form of communication networks, see Fig. 1, which is significantly different from traditional point-to-point control systems whose components are attached directly to the physical plant. Compared with traditional control systems, main merits of NCSs come from their modular and flexible system design, fast implementation, and distribution [1]–[3]. Consequently, NCSs have been widely used nowadays in spacecrafts, industrial manufacturing processes, vehicles and other complicated control systems [4], [5]. But some disadvantages such as time delay in data transmission may also degrade the closed-loop system performance and should be fully used in the design procedure. The key issue of NCSs is how to deal with the network-induced delay including the sensor-to-controller τ_{sc} and the controller-to-actuator τ_{ca}. A common model for NCSs subject to network-induced delays consists of a continuous-time plant and a discrete-time controller [1], [3], [4], [7], in which both the sensor-to-controller delay τ_{sc} and the controller-to-actuator one τ_{ca} are lumped together as $\tau = \tau_{sc} + \tau_{ca}$ for performance analysis purposes. The closed-loop form of NCSs is generally modeled as sampled-data control systems [7].

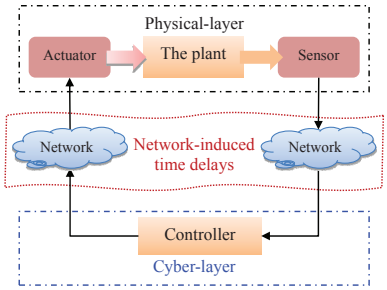

Fig. 1: The schematic map of networked control systems [1]

On the other hand, industrial control processes have severe nonlinear characteristics [3], [6], which make their design and performance analysis more difficult. It has been shown from considerable theoretical/applied research results that fuzzy control, especially Takagi-Sugeno (T-S) fuzzy-model-based control [8], offers an effective framework to deal with the control synthesis problem of complex dynamic systems [9]–[13]. Over the past few decades, with the aid of fuzzy model, fruitful results of analysis and synthesis have been reported for nonlinear NCSs [3], [14]–[19] and nonlinear sampled-data control system [20]–[25], whose system dynamics only depends on time and mathematical model is represented by ordinary differential-difference equations (ODdEs). Despite the above gratifying progress, practical engineering applications raise a class of more complex dynamic processes with spatiotemporal dynamic behaviors [26]–[30], which are completely distinct from the ones discussed in [3], [14]–[25]. Such complex spatiotemporal dynamic processes are modeled by partial differential equations (PDEs) and referred to be distributed parameter systems (DPSs). In this article, we will deal with the nonlinear spatiotemporal feedback compensator

This work was supported in part by High-Level Foreign Experts Introduction Plan under Grant G2022105025L, in part by National Natural Science Foundation of China under Grants 92271115, 62203161 and in part by Beijing Natural Science Foundation under Grant 4192037. *Corresponding Author: Yun Feng*

Jun-Wei Wang is with the School of Intelligent Science and Technology, University of Science and Technology Beijing, Beijing 100083, P. R. China, e-mail: junweiwang@ustb.edu.cn.

Yun Feng is with the College of Electrical and Information Engineering, Hunan University, Changsha 410082, China, and also with the National Engineering Research Center for Robot Visual Perception and Control Technology, Hunan University, Changsha 410082, China, email: fyrobot@hnu.edu.cn.

Stevan Dubljevic is with the Department of Chemical & Materials Engineering, University of Alberta, Canada, e-mail: Stevan.Dubljevic@ualberta.ca.

Hak-Keung Lam is with the Department of Engineering, King's College London Strand, London, U.K., e-mail: hak-keung.lam@kcl.ac.uk.

design for nonlinear networked parabolic PDE systems by the spatiotemporal T-S fuzzy-model-based control technique.

B. Literature Review and Discussion

Recently, numerous researchers have paid attention to the investigation of nonlinear NCSs [3], [14]–[19]. Shen *et al.* [15] have addressed the issue of reliable output feedback control for nonlinear networked semi-Markov jump systems via the fuzzy-model-based control method and proposed a control strategy with redundant channels to reduce the adverse effect caused by packet dropouts. Lian *et al.* [16] have discussed the problem of dynamic hybrid-triggered control for nonlinear networked control systems and developed a resilient control scheme to improve network resource utilization and system performance against cyberattacks for the underlying systems. In [18], the authors have proposed an event-based static output feedback fuzzy tracking control scheme for discrete-time nonlinear networked systems subject to dynamic quantization. Sun *et al.* [19] have discussed security control of T-S fuzzy networked systems subject to cyberattacks and successive packet losses in the sensor-controller and controller-actuator channels.

Due to the fact that the closed-loop form of NCSs can be modeled as sampled-data control systems [1], [7], the issue of sampled-data/event-triggered control system design and performance analysis have received a great deal of attention from the control system community [20]–[25]. In [22], the issue of event-triggered state feedback control has been addressed for interval type-2 fuzzy systems subject to the fading channel. An input delay approach has been adopted in [23] to address the sampled-data output-feedback control issue for nonlinear systems represented by T-S fuzzy affine models. Wang and Yang [24] have dealt with the issue of robust filtering for continuous-time T-S fuzzy systems with bounded external disturbances via premise-region-dependent event-triggered mechanisms. In [25], an improved fuzzy-dependent adaptive event-triggered mechanism has been discussed for sampled-data-based control of T-S fuzzy systems. It must be pointed out that the complex dynamics of nonlinear plants in the above works are modeled by T-S fuzzy ordinary differential equation (ODE) model.

For the sampled-data control design of DPSs, some effective methods have been reported in [31]–[41]. For example, by resorting to the modal decomposition technique, some finite-dimensional sampled-data control designs were reported for parabolic PDE systems [31]–[34]. However, notice that the model truncation before control design in the finite-dimensional control design may result in an inaccurate control performance. To overcome such drawback, PDE-based design methods were developed for linear sampled-data controllers of semi-linear parabolic systems [35]–[38]. In [39]–[41], an infinite-dimensional nonlinear sampled-data control design has been recently developed via the exact T-S fuzzy PDE model. Note that the design methods in [39]–[41] were developed under a strong assumption that control actions cover the entire spatial domain. This strong assumption was removed in [42], [43] by resorting to the observer-based output feedback control technique. More recently, event-triggered fuzzy control schemes have been reported in [44]–[46] for semi-linear parabolic PDE systems. Moreover, the exact T-S fuzzy model proposed in [39]–[41], [44]–[46] requires the precise dynamics of the nonlinear PDEs. Generally, it is very difficult to obtain the precise system dynamics for real application problems. Hence, the study on infinite-dimensional fuzzy-model-based feedback compensator design is very necessary for sampled-data/networked parabolic PDE systems with local piecewise control and imprecise nonlinear dynamics, which motivates the present work.

C. Main Results and Technical Contributions of This Article

In this study, on the basis of the authors' previous works [39], [42], [43], we further deal with the problem of infinite-dimensional fuzzy-model-based feedback compensator design for nonlinear parabolic PDE systems with local piecewise control and measurement outputs over network. The new features and novelties of this study are summarized as follows

1) *Lyapunov-based Spatiotemporal Fuzzy Control Design of Networked Parabolic PDE Systems*: In the observer-based feedback control framework, a Lyapunov-based design of spatiotemporal fuzzy continuous-time and sampled-data compensators is solved for parabolic PDE systems with local piecewise control and the networked measurement outputs. The main results are presented in terms of standard linear matrix inequalities (LMIs) and are checked by the *feasp* solver in MATLAB's LMI Control Toolbox [47].
2) *Networked Parabolic PDE Systems*: Different from the existing networked control systems [3], [4], [7], [15]–[19], where the complex system dynamic behaviour is modeled by ODEs, the main difficulty of feedback control design for networked parabolic PDE systems lies in the spatiotemporal evolution dynamics described by sampled-data parabolic PDEs.
3) *Approximate Spatiotemporal T-S Fuzzy Model*: Compared to the exact fuzzy model in [33], [34], [39]–[41], [44]–[46], [48], [49], this article proposes an approximate T-S fuzzy PDE model with C^{∞}-smooth membership functions for the representation of complex nonlinear spatiotemporal evolution dynamics of parabolic PDE systems. Different from the work [50], this article analyzes the approximation performance of the suggested approximate T-S fuzzy model via the uniform approximation theorem for continuous functions on a real separable Hilbert space.

D. Organization and Notation

Organization: Section II formulates the control design problem addressed in this article, which includes system description of nonlinear parabolic dynamic systems, approximate T-S fuzzy PDE model and its approximation capability analysis, and the spatiotemporal fuzzy-observer-based nonlinear compensator's structure. Section III constructs two types of fuzzy-observer-based feedback compensators (i.e., continuous-time control and sampled-data control) via the networked measurement outputs. Numerical simulation results are presented in Section IV to validate the effectiveness and merit of the

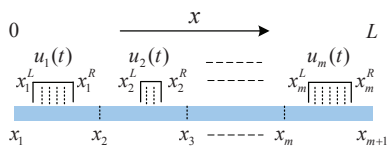

Fig. 2: Sampled-data control in space

proposed fuzzy compensators. Finally, Section V provides some brief concluding discussions.

Notation: $\Re$, $\Re^n$ and $\Re^{m\times n}$ are respectively used for sets of real numbers, n-dimensional Euclidean space, and $m\times n$ matrices. For a given scalar $L>0$, $\mathcal{L}_n^2([0,L])\triangleq\mathcal{L}^2([0,L];\Re^n)$ is a ***separable*** Hilbert space of square integrable vector functions $\boldsymbol{\zeta}(x)$ with $\|\boldsymbol{\zeta}(\cdot)\|_2 \triangleq \sqrt{\int_0^L \boldsymbol{\zeta}^T(x)\boldsymbol{\zeta}(x)dx}$. $\mathcal{H}_n^{\bar{k}}((0,L)) \triangleq \mathcal{W}^{\bar{k},2}((0,L);\Re^n)$ is a Sobolev space of absolutely continuous vector functions $\boldsymbol{\zeta}(x)$ with square integrable derivatives $\frac{d^{\bar{k}}\boldsymbol{\zeta}(x)}{dx^{\bar{k}}}$ of the order $\bar{k}$ (a given integer) and $\|\boldsymbol{\zeta}(\cdot)\|_{\mathcal{H}_n^{\bar{k}}((0,L))} \triangleq \sqrt{\int_0^L \sum_{i=0}^{\bar{k}} \frac{d^i\boldsymbol{\omega}^T(x)}{dx^i}\frac{d^i\boldsymbol{\zeta}(x)}{dx^i}dx}$. For $\boldsymbol{\varpi}(\cdot,t)\in\mathcal{H}_n^2((0,L))$, the partial derivatives $\partial\boldsymbol{\varpi}(x,t)/\partial t$ and $\partial\boldsymbol{\varpi}(x,t)/\partial x$ are denoted by $\boldsymbol{\varpi}_t(x,t)$ and $\boldsymbol{\varpi}_x(x,t)$, respectively. The transpose operation is denoted by the superscript 'T' for a vector or a matrix. A block diagonal matrix created by M matrices $\boldsymbol{C}_i$, $i\in\{1,2,\cdots,M\}$ is denoted by Block-diag$\{\boldsymbol{C}_1,\boldsymbol{C}_2,\cdots,\boldsymbol{C}_M\}$.

II. Problem Formulation

A. System description

This article considers a nonlinear parabolic dynamic system

$$\begin{cases} \boldsymbol{z}_t(x,t)=\boldsymbol{\Theta}\boldsymbol{z}_{xx}(x,t)+\boldsymbol{f}(\boldsymbol{z}(x,t))+\boldsymbol{G}(x)\boldsymbol{u}(t), \\ \qquad\qquad\qquad\qquad x\in(0,L),\ t>t_0, \\ \boldsymbol{z}(0,t)=\boldsymbol{z}(L,t)=0,\ t\geq t_0, \\ \boldsymbol{z}(x,t_0)=\boldsymbol{z}_0(x),\ x\in[0,L], \end{cases} \tag{1}$$

where $\boldsymbol{z}(x,t)\triangleq[z_1(x,t)\quad z_2(x,t)\quad\cdots\quad z_n(x,t)]^T\in\mathbb{D}$ is the state ($\mathbb{D}$ is an open subset of $\mathcal{L}_n^2([0,L])$ and contains the equilibrium profile $\boldsymbol{z}(\cdot,t)=0$), $x\in[0,L]\subset\Re$ and $t\geq t_0$ (t_0 is the initial time) are spatial position and time coordinates, respectively. The diffusion coefficient matrix $0<\boldsymbol{\Theta}\in\Re^{n\times n}$ is known, and the nonlinear function $\boldsymbol{f}(\boldsymbol{z})$ with $\boldsymbol{f}(0)=0$ is continuous with respect to $\boldsymbol{z}$. The integrable matrix function $\boldsymbol{G}(x)\triangleq[\boldsymbol{g}_1(x)\quad\boldsymbol{g}_2(x)\quad\cdots\quad\boldsymbol{g}_m(x)]\in\Re^{n\times m}$ with

$$\boldsymbol{g}_\kappa(x)\triangleq\begin{cases}\frac{\boldsymbol{g}_\kappa}{\Delta x_\kappa} & x\in[x_\kappa^L,x_\kappa^R],\\ 0 & \text{otherwise},\end{cases}\quad \kappa\in\mathfrak{M}, \tag{2}$$

in which $\Delta x_\kappa\triangleq x_\kappa^R-x_\kappa^L$, $\mathfrak{M}\triangleq\{1,2,\cdots,m\}$ model the distribution of m actuators over $(0,L)$, $[x_\kappa^L,x_\kappa^R]$ is the κ-th actuator's active area. These actuators provide the control input $\boldsymbol{u}(t)\triangleq[u_1(t)\quad u_2(t)\quad\cdots\quad u_m(t)]^T\in\Re^m$. The chosen function $\boldsymbol{G}(x)$ produces m zones of *spatially sampled-data control* over $[x_\kappa^L,x_\kappa^R]$, $\kappa\in\mathfrak{M}$ (see Fig. 2).

Remark 1: Define $\boldsymbol{\mathcal{A}}\bar{\boldsymbol{y}}(x)\triangleq\boldsymbol{\Theta}\frac{d^2\bar{\boldsymbol{y}}(x)}{dx^2}$ with $\mathcal{D}(\boldsymbol{\mathcal{A}})\triangleq\{\bar{\boldsymbol{y}}\in\mathcal{H}_n^2((0,L)):\bar{\boldsymbol{y}}(0)=\bar{\boldsymbol{y}}(L)=0\}$. Since $\boldsymbol{\mathcal{A}}$ is a linear, symmetric, and compact operator in $\mathcal{L}_n^2([0,L])$, its eigenvalue problem $\boldsymbol{\mathcal{A}}\tilde{\boldsymbol{y}}_\iota(x)=\lambda_\iota\tilde{\boldsymbol{y}}_\iota(x)$, $\iota\in\{1,2,\cdots,\infty\}$ can be solved analytically. All real eigenvalues λ_ι are ordered (i.e., $\lambda_{\iota+1}\leq\lambda_\iota$) and the eigenfunctions $\tilde{\boldsymbol{y}}_\iota(x)$ form an orthonormal basis for $\mathcal{D}(\boldsymbol{\mathcal{A}})$. For example, if $\boldsymbol{\Theta}$ is an identify one and the eigenfunction $\tilde{\boldsymbol{y}}_\iota(x)$ is chosen as $\sqrt{\frac{2}{L}}\sin(\iota\pi L^{-1}x)[1\quad 1\quad\cdots\quad 1_n]^T\in\Re^n$, then the eigenvalue is $\lambda_\iota=-\frac{\iota^2\pi^2}{L^2}$. By the Hilbert-Schmidt theorem [51], the eigenfunctions $\tilde{\boldsymbol{y}}_\iota(x)$, $\iota\in\{1,2,\cdots,\infty\}$ constitute a set of bases for $\mathcal{L}_n^2([0,L])$. That is, $\mathcal{L}_n^2([0,L])$ is ***separable***.

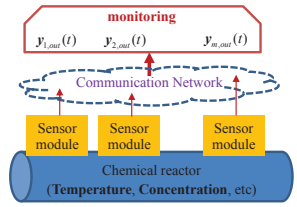

Fig. 3: Industrial-internet-based remote monitoring of chemical reaction process

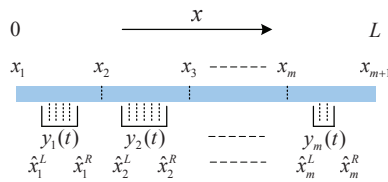

Fig. 4: Asynchronous sampled-data observation in space

The measurement outputs $\boldsymbol{y}_{\kappa,out}(t)$, $\kappa\in\mathfrak{M}$ are transmitted over the communication network (see Fig. 3). Due to the network-induced time delays, the networked measurement outputs can be modeled by the following sampled-data measurement output equations

$$\boldsymbol{y}_{\kappa,out}(t)=\int_0^L c_\kappa(x)\boldsymbol{z}(x,t_k)dx,\ \kappa\in\mathfrak{M},$$
$$t\in[t_k,t_{k+1}),\ k\in\mathfrak{N}\triangleq\{0,1,2,\cdots\}, \tag{3}$$

where $c_\kappa(x)$ is defined as

$$c_\kappa(x)\triangleq\begin{cases}(\Delta\hat{x}_\kappa)^{-1} & x\in[\hat{x}_\kappa^L\hat{x}_\kappa^R],\\ 0 & \text{otherwise},\end{cases} \tag{4}$$

with $\Delta\hat{x}_\kappa\triangleq\hat{x}_\kappa^R-\hat{x}_\kappa^L$, which produces the spatially sampled-data observation over $[\hat{x}_\kappa^L,\hat{x}_\kappa^R]$, $\kappa\in\mathfrak{M}$ (see Fig. 4). The measurement output signals $\boldsymbol{y}_{\kappa,out}(t)$, $\kappa\in\mathfrak{M}$ are kept constant during the sampling period $[t_k,t_{k+1})$, $k\in\mathfrak{N}$ via the zero-order holder (ZOH) and are allowed to change only at the sampling moments t_k, $k\in\mathfrak{N}$, in which $t_{k+1}-t_k\leq T_o$, $k\in\mathfrak{N}$ and $T_o>0$ is a constant given in advance. Note that the sampling between control and observation is ***spatiotemporally asynchronous*** as $[x_\kappa^L,x_\kappa^R]\neq[\hat{x}_\kappa^L,\hat{x}_\kappa^R]$, $\kappa\in\mathfrak{M}$ and the asynchronous sampling in time between control input and observation output.

Remark 2: The PDE model (1) with the spatiotemporally asynchronous sampled-data measurement outputs (3) can be used to describe the complex dynamic behaviour of the industrial-internet-based remote monitoring of a class of industrial process subject to reaction-diffusion phenomena (e.g., thermal diffusion processes, chemical processes, and oil plume

propagation, etc). The measurement outputs of the industrial process are transmitted over the industrial network and are provided by some sensors active over some local areas of spatial domain, whose distribution in the spatial domain $(0, L)$ can be modeled by the equation (4).

B. Approximate T-S fuzzy PDE model and its approximation capability analysis

A T-S fuzzy PDE model of the following form is given to approximate the complex spatiotemporal dynamics of the semi-linear PDE in (1):

Model Rule i**:**

IF ζ_1 is M_{i1} and $\cdots$ and ζ_d is M_{id}, **THEN**

$$\begin{aligned} \boldsymbol{z}_t(x,t) = \boldsymbol{\Theta}\boldsymbol{z}_{xx}(x,t) + \boldsymbol{A}_i\boldsymbol{z}(x,t) + \boldsymbol{G}(x)\boldsymbol{u}(t), \\ x \in (0,L),\ t > t_0,\ i \in \mathfrak{S}, \end{aligned} \tag{5}$$

where ζ_j and M_{ij}, $i \in \mathfrak{S} \triangleq \{1, 2, \cdots, s\}$, $j \in \{1, 2, \cdots, d\}$ are premise variables and fuzzy sets, respectively, $\boldsymbol{A}_i \in \Re^{n\times n}$, $i \in \mathfrak{S}$, and s is the fuzzy rule number. We assume that the premise variables are functions of $\boldsymbol{z}$ and represented by $\zeta_j(\boldsymbol{z})$.

For any $i \in \mathfrak{S}$, $j \in \{1, 2, \cdots, d\}$, the grade of the membership of $\zeta_j(\boldsymbol{z})$ in M_{ij} is denoted by $O_{ij}(\zeta_j(\boldsymbol{z}))$. Define $\boldsymbol{\zeta}(\boldsymbol{z}) \triangleq [\zeta_1(\boldsymbol{z}) \quad \zeta_2(\boldsymbol{z}) \quad \cdots \quad \zeta_d(\boldsymbol{z})]^T$ and $w_i(\boldsymbol{\zeta}(\boldsymbol{z})) \triangleq \frac{\prod_{j=1}^{d} O_{ij}(\zeta_j(\boldsymbol{z}))}{\sum_{i=1}^{s}\prod_{j=1}^{d} O_{ij}(\zeta_j(\boldsymbol{z}))}$, $i \in \mathfrak{S}$. For any $i \in \mathfrak{S}$, we assume $\prod_{j=1}^{d} O_{ij}(\zeta_j(\boldsymbol{z})) > 0$, which means that

$$w_i(\boldsymbol{\zeta}(\boldsymbol{z})) \geq 0,\ i \in \mathfrak{S} \text{ and } \sum_{i=1}^{s} w_i(\boldsymbol{\zeta}(\boldsymbol{z})) = 1. \tag{6}$$

Via the fuzzy membership functions in (6), the overall dynamic expression of the above fuzzy PDE model is given by

$$\begin{aligned} \boldsymbol{z}_t(x,t) = \boldsymbol{\Theta}\boldsymbol{z}_{xx}(x,t) + \sum_{i=1}^{s} w_i(\boldsymbol{\zeta}(\boldsymbol{z}))\boldsymbol{A}_i\boldsymbol{z}(x,t) \\ + \boldsymbol{G}(x)\boldsymbol{u}(t), \quad x \in (0,L),\ t > t_0, \end{aligned} \tag{7}$$

which can be interpreted as an interpolation of s linear PDEs via the membership functions $w_i(\boldsymbol{\zeta}(\boldsymbol{z}))$ to approximate the PDE in (1). Hence, the PDE in (1) is rewritten as

$$\begin{aligned} \boldsymbol{z}_t(x,t) = \boldsymbol{\Theta}\boldsymbol{z}_{xx}(x,t) + \sum_{i=1}^{s} w_i(\boldsymbol{\zeta}(\boldsymbol{z}))\boldsymbol{A}_i\boldsymbol{z}(x,t) + \boldsymbol{G}(x)\boldsymbol{u}(t) \\ + \Delta\boldsymbol{f}(\boldsymbol{z}(x,t)),\ x \in (0,L),\ t > t_0, \end{aligned} \tag{8}$$

where $\Delta\boldsymbol{f}(\boldsymbol{z}(x,t)) \triangleq \boldsymbol{f}(\boldsymbol{z}(x,t)) - \sum_{i=1}^{s} w_i(\boldsymbol{\zeta}(\boldsymbol{z}))\boldsymbol{A}_i\boldsymbol{z}(x,t)$ is the approximation error of the fuzzy PDE model (7). Obviously, the error $\Delta\boldsymbol{f}(\boldsymbol{z})$ depends on the fuzzy rule number s and is used to measure the performance of the fuzzy model (7).

To analyze the approximation capability of the T-S fuzzy PDE model (7), we make the following assumption for the membership function $w_i(\boldsymbol{\zeta}(\boldsymbol{z}))$ in (7):

Assumption 1: For any $i \in \mathfrak{S}$, the membership function $w_i(\boldsymbol{\zeta}(\boldsymbol{z}))$ is a C^∞-smooth mapping in $\boldsymbol{\zeta}$.

Under Assumption 1, the fuzzy PDE model (7) is C^∞-smooth in $\boldsymbol{z}(x,t)$. By Lemma 2 [52], for every continuous function $\boldsymbol{f}(\boldsymbol{z})$ defined on the open subset $\mathbb{D}$ and every continuous positive function $\varepsilon(\boldsymbol{z})$, there exists a C^∞-smooth fuzzy mapping $\sum_{i=1}^{s} w_i(\boldsymbol{\zeta}(\boldsymbol{z}))\boldsymbol{A}_i\boldsymbol{z}$ such that $(\Delta\boldsymbol{f}(\boldsymbol{z}))^T\Delta\boldsymbol{f}(\boldsymbol{z}) < \varepsilon(\boldsymbol{z})$ is fulfilled for all $\boldsymbol{z} \in \mathbb{D}$. Without loss of generality, Assumption 2 is thus made for the approximation error $\Delta\boldsymbol{f}(\boldsymbol{z})$.

Assumption 2: There is a scalar $\varepsilon > 0$ such that the inequality $(\Delta\boldsymbol{f}(\boldsymbol{z}))^T\Delta\boldsymbol{f}(\boldsymbol{z}) < \varepsilon\boldsymbol{z}^T\boldsymbol{z}$ holds for all $\boldsymbol{z} \in \mathbb{D}$.

Remark 3: Assumption 2 only ensures the existence of the constant $\varepsilon > 0$. A natural question arises in the analysis of fuzzy control design. One may ask how to determine the specific value of $\varepsilon > 0$. A practical and feasible method for determining the value of $\varepsilon > 0$ is to define $\varepsilon \triangleq \sup_{\boldsymbol{z}\in\mathbb{D}}\left\{\frac{(\Delta\boldsymbol{f}(\boldsymbol{z}))^T\Delta\boldsymbol{f}(\boldsymbol{z})}{\boldsymbol{z}^T\boldsymbol{z}}\right\}$ for a given fuzzy rule number s, which can be approximately calculated via the interpolation method. On the other hand, the approximate fuzzy PDE model (e.g., the value of the fuzzy rule number s) can be optimized via the least-square method by minimizing the error $\Delta\boldsymbol{f}(\boldsymbol{z})$ [50].

C. Problem formulation

To estimate the spatiotemporal coupling state $\boldsymbol{z}(x,t)$ of the PDE model (1), the following Luenberger-type PDE state observer is constructed via the T-S fuzzy PDE model (5)

Observer Rule q**:**

IF $\hat{\zeta}_1$ is M_{q1} and $\cdots$ and $\hat{\zeta}_d$ is M_{qd}, **THEN**

$$\begin{aligned} \hat{\boldsymbol{z}}_t(x,t) = \boldsymbol{\Theta}\hat{\boldsymbol{z}}_{xx}(x,t) + \boldsymbol{A}_i\hat{\boldsymbol{z}}(x,t) + \boldsymbol{G}(x)\boldsymbol{u}(t) \\ + \boldsymbol{L}_{\kappa q}[\boldsymbol{y}_{\kappa,out}(t) - \hat{\boldsymbol{y}}_{\kappa,out}(t)], \\ x \in (x_\kappa, x_{\kappa+1}),\ t > t_0,\ q \in \mathfrak{S},\ \kappa \in \mathfrak{M}, \end{aligned} \tag{9}$$

where $\boldsymbol{L}_{\kappa q}$ is the observer gain for the q-th observation rule ($q \in \mathfrak{S}$ and $\kappa \in \mathfrak{M}$), the premise variables $\hat{\zeta}_j$, $j \in \{1, 2, \cdots, d\}$ are functions of $\hat{\boldsymbol{z}}$ and represented by $\hat{\zeta}_j(\hat{\boldsymbol{z}})$, the boundary estimate $\hat{\boldsymbol{z}}(0,t) = \hat{\boldsymbol{z}}(L,t) = 0$, $t \geq t_0$, the initial estimate $\hat{\boldsymbol{z}}(x,t_0) = \hat{\boldsymbol{z}}_0(x)$, $x \in [0,L]$, the observer outputs $\hat{\boldsymbol{y}}_{\kappa,out}(t) = \int_0^L c_\kappa(x)\hat{\boldsymbol{z}}(x,t_k)dx$, $\kappa \in \mathfrak{M}$, $t \in [t_k, t_{k+1})$, $k \in \mathfrak{N}$, and $[\hat{x}_\kappa^L, \hat{x}_\kappa^R] \subset (x_\kappa, x_{\kappa+1})$, $\kappa \in \mathfrak{M}$ (see Fig. 2). The overall fuzzy PDE observer (9) is expressed as

$$\begin{aligned} \hat{\boldsymbol{z}}_t(x,t) = \boldsymbol{\Theta}\hat{\boldsymbol{z}}_{xx}(x,t) + \sum_{q=1}^{s} w_q(\hat{\boldsymbol{\zeta}}(\hat{\boldsymbol{z}}))\boldsymbol{A}_q\hat{\boldsymbol{z}}(x,t) + \boldsymbol{G}(x)\boldsymbol{u}(t) \\ + \sum_{q=1}^{s} w_q(\hat{\boldsymbol{\zeta}}(\hat{\boldsymbol{z}}))\boldsymbol{L}_{\kappa q}[\boldsymbol{y}_{\kappa,out}(t) - \hat{\boldsymbol{y}}_{\kappa,out}(t)], \\ x \in (x_\kappa, x_{\kappa+1}),\ t > t_0,\ \kappa \in \mathfrak{M}, \end{aligned} \tag{10}$$

where $\hat{\boldsymbol{\zeta}}(\hat{\boldsymbol{z}}) \triangleq [\hat{\zeta}_1(\hat{\boldsymbol{z}}) \quad \hat{\zeta}_2(\hat{\boldsymbol{z}}) \quad \cdots \quad \hat{\zeta}_d(\hat{\boldsymbol{z}})]^T$ and $w_q(\hat{\boldsymbol{\zeta}}(\hat{\boldsymbol{z}}))$, $q \in \mathfrak{S}$ satisfy

$$w_q(\hat{\boldsymbol{\zeta}}(\hat{\boldsymbol{z}})) \geq 0,\ q \in \mathfrak{S} \text{ and } \sum_{q=1}^{s} w_q(\hat{\boldsymbol{\zeta}}(\hat{\boldsymbol{z}})) = 1. \tag{11}$$

In the subsequent statements, $w_i(\boldsymbol{\zeta}(\boldsymbol{z}))$ and $w_q(\hat{\boldsymbol{\zeta}}(\hat{\boldsymbol{z}}))$ are respectively denoted by $w_i(\boldsymbol{\zeta})$ and $w_q(\hat{\boldsymbol{\zeta}})$ for brevity.

The corresponding estimation error $\boldsymbol{e}(x,t)$ is defined by

$$\boldsymbol{e}(x,t) \triangleq \boldsymbol{z}(x,t) - \hat{\boldsymbol{z}}(x,t), \tag{12}$$

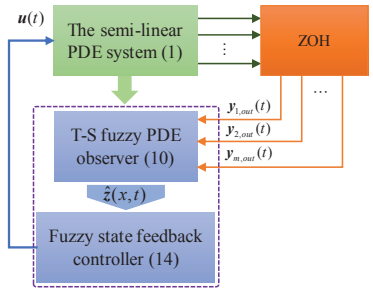

Fig. 5: A schematic diagram of the spatiotemporal fuzzy-observer-based nonlinear continuous-time compensator (14) with (10) and networked measurement outputs modeled by sampled-data equation (3)

which is subject to

$$\begin{cases} \boldsymbol{e}_t(x,t) = \boldsymbol{\Theta}\boldsymbol{e}_{xx}(x,t) + \sum_{q=1}^{s} w_q(\hat{\boldsymbol{\zeta}})\boldsymbol{A}_q\boldsymbol{e}(x,t) + \Delta\boldsymbol{f}(\boldsymbol{z}(x,t)) \\ \qquad + \sum_{i,q=1}^{s} w_i(\boldsymbol{\zeta})w_q(\hat{\boldsymbol{\zeta}})[\boldsymbol{A}_i - \boldsymbol{A}_q]\boldsymbol{z}(x,t) \\ \qquad - \sum_{q=1}^{s} w_q(\hat{\boldsymbol{\zeta}})\boldsymbol{L}_{\kappa q}\int_0^L c_\kappa(x)\boldsymbol{e}(x,t_k)dx, \\ \qquad k \in \mathfrak{N},\ x \in (x_\kappa, x_{\kappa+1}),\ t > t_0,\ \kappa \in \mathfrak{M}, \\ \boldsymbol{e}(0,t) = \boldsymbol{e}(L,t) = 0,\ t \geq t_0, \\ \boldsymbol{e}(x,t_0) = \boldsymbol{e}_0(x),\ x \in [0,L]. \end{cases} \tag{13}$$

On the basis of the fuzzy model (8) with Assumptions 1 and 2, the aim of the present study is to propose an effective design method of the spatiotemporal fuzzy-observer-based nonlinear feedback compensators for the semi-linear parabolic system (1) such that the exponential stability of the resulting closed-loop augmented fuzzy PDE system.

III. Spatiotemporal Fuzzy-Observer-Based Compensators via Networked Measurements

Two types of spatiotemporal fuzzy compensators (i.e., continuous-time control and sampled-data control) are constructed in this section via the networked measurement outputs modeled by sampled-data equation (3). The continuous-time control method is applicable to the case when control signals are fed to actuators directly, while the sampled-data control approach can be used to solve the case when control signals are transmitted over networks.

A. Continuous-time control

A fuzzy state feedback controller is proposed via the estimated spatiotemporal coupling state $\hat{\boldsymbol{z}}(x,t)$

$$u_\kappa(t) = \sum_{q=1}^{s}\int_{x_\kappa}^{x_{\kappa+1}} w_q(\hat{\boldsymbol{\zeta}})\boldsymbol{k}_{\kappa q}^T\hat{\boldsymbol{z}}(x,t)dx,\ \kappa \in \mathfrak{M}, \tag{14}$$

in which the parameters $\boldsymbol{k}_{\kappa q} \in \Re^n$, $\kappa \in \mathfrak{M}$, $q \in \mathfrak{S}$ are to be determined, and $[x_\kappa^L, x_\kappa^R] \subset (x_\kappa, x_{\kappa+1})$, $\kappa \in \mathfrak{M}$ ($\bigcup_{\kappa\in\mathfrak{M}}[x_\kappa, x_{\kappa+1}] = [0,L]$, see Fig. 2). Fig. 5 provides a schematic diagram of the proposed spatiotemporal fuzzy-observer-based feedback controller via networked measurement outputs modeled by sampled-data equation (3).

By substituting the fuzzy controller (14) into the fuzzy PDE model (8) and considering $\boldsymbol{G}(x)$ in (2), and (12), we get the resulting closed-loop augmented fuzzy PDE system as the form (13) and the following PDE:

$$\begin{cases} \boldsymbol{z}_t(x,t) = \boldsymbol{\Theta}\boldsymbol{z}_{xx}(x,t) + \sum_{i=1}^{s} w_i(\boldsymbol{\zeta})\boldsymbol{A}_i\boldsymbol{z}(x,t) + \Delta\boldsymbol{f}(\boldsymbol{z}(x,t)) \\ \qquad + \boldsymbol{g}_\kappa(x)\int_{x_\kappa}^{x_{\kappa+1}}\sum_{q=1}^{s} w_q(\hat{\boldsymbol{\zeta}})\boldsymbol{k}_{\kappa q}^T[\boldsymbol{z}(x,t) - \boldsymbol{e}(x,t)]dx, \\ \qquad x \in (0,L),\ t > t_0,\ \kappa \in \mathfrak{M}, \\ \boldsymbol{z}(0,t) = \boldsymbol{z}(L,t) = 0,\ t \geq t_0, \\ \boldsymbol{z}(x,t_0) = \boldsymbol{z}_0(x),\ x \in [0,L]. \end{cases} \tag{15}$$

Definition 1 ([48], [49]): The resulting closed-loop fuzzy coupled PDEs (13) and (15) are exponentially stable in the sense of $\|\cdot\|_2$ if $\sqrt{\|\boldsymbol{z}(\cdot,t)\|_2^2 + \|\boldsymbol{e}(\cdot,t)\|_2^2} \leq \beta_1\exp(-\beta_2 t)$, where $\beta_1 > 0$ and $\beta_2 > 0$ are two known constants.

Consider a Lyapunov–Krasovskii functional candidate for the closed-loop augmented fuzzy PDE system (13) and (15):

$$V(t) = V_0(t) + V_1(t) + V_2(t) + V_3(t),\ t \in [t_k, t_{k+1}),\ k \in \mathfrak{N}, \tag{16}$$

where

$$V_0(t) = \nu\int_0^L \boldsymbol{z}^T(x,t)\boldsymbol{P}_1\boldsymbol{z}(x,t)dx, \tag{17}$$

$$V_1(t) = \int_0^L \boldsymbol{e}^T(x,t)\boldsymbol{P}_1\boldsymbol{e}(x,t)dx, \tag{18}$$

$$V_2(t) = \int_0^L \boldsymbol{e}_x^T(x,t)\boldsymbol{P}_2\boldsymbol{e}_x(x,t)dx, \tag{19}$$

$$V_3(t) = T_o\int_0^L\int_{t_k}^{t}(s - t + T_o)\boldsymbol{e}_s^T(x,s)\boldsymbol{P}_3\boldsymbol{e}_s(x,s)dsdx, \tag{20}$$

with $\nu > 0$ is a given design parameter, and $0 < \boldsymbol{P}_j$, $j \in \{1,2,3\}$ are $n \times n$ Lyapunov matrices to be determined.

Theorem 1: Consider the semi-linear PDE system (1)-(4) and the approximate fuzzy model (8) with Assumptions 1 and 2. Given an integer $m > 0$, some constants $L > 0$, $T_o > 0$, x_κ^L, x_κ^R, $\hat{x}_\kappa^L$, $\hat{x}_\kappa^R$, x_κ, $\kappa \in \mathfrak{M}$, and x_{m+1} ($0 = x_1 < x_2 < x_3 < \cdots < x_m < x_{m+1} = L$, $[x_\kappa^L, x_\kappa^R] \subset (x_\kappa, x_{\kappa+1})$, and $[\hat{x}_\kappa^L, \hat{x}_\kappa^R] \subset (x_\kappa, x_{\kappa+1})$, $\kappa \in \mathfrak{M}$) and design parameters $\nu > 0$, $\sigma > 0$, and $\varepsilon > 0$ (Assumption 2), if there exist matrices $0 < \boldsymbol{X}_j \in \Re^{n\times n}$, $j \in \{1,2,3\}$, $\boldsymbol{Y}_{\kappa q} \in \Re^{n\times n}$ and vectors $\boldsymbol{o}_{\kappa q} \in \Re^n$, $\kappa \in \mathfrak{M}$, $q \in \mathfrak{S}$ satisfying the following LMIs:

$$\boldsymbol{\Phi}_1 \triangleq [\boldsymbol{\Theta}\boldsymbol{X}_1 + *] > 0, \tag{21}$$

$$\boldsymbol{\Phi}_{\kappa iq} \triangleq \begin{bmatrix} \nu\boldsymbol{\Phi}_{1\kappa iq} & \boldsymbol{\Phi}_{4\kappa iq} & \boldsymbol{\Phi}_{7iq} & \boldsymbol{\Phi}_9 & \boldsymbol{\Phi}_{10} \\ \boldsymbol{\Phi}_{4\kappa iq}^T & \boldsymbol{\Phi}_{2\kappa q} & \boldsymbol{\Phi}_{5\kappa q} & \boldsymbol{\Phi}_8 & 0 \\ \boldsymbol{\Phi}_{7iq}^T & \boldsymbol{\Phi}_{5\kappa q}^T & \boldsymbol{\Phi}_{3\kappa q} & \boldsymbol{\Phi}_6 & 0 \\ \boldsymbol{\Phi}_9^T & \boldsymbol{\Phi}_8^T & \boldsymbol{\Phi}_6^T & -\sigma\boldsymbol{I} & 0 \\ \boldsymbol{\Phi}_{10}^T & 0 & 0 & 0 & -\frac{\boldsymbol{I}}{\sigma\varepsilon} \end{bmatrix} < 0, \\ \kappa \in \mathfrak{M},\ i,q \in \mathfrak{S}, \tag{22}$$

where $\boldsymbol{I}$ is an identity matrix of appropriate dimension, and

$$\boldsymbol{\Phi}_{1\kappa iq} \triangleq \begin{bmatrix} [\boldsymbol{A}_i\boldsymbol{X}_1 + *] - \frac{\pi^2}{4\varphi_\kappa}\boldsymbol{\Phi}_1 & \frac{\pi^2}{4\varphi_\kappa}\boldsymbol{\Phi}_1 + \boldsymbol{g}_\kappa\boldsymbol{o}_{\kappa q}^T \\ \frac{\pi^2}{4\varphi_\kappa}\boldsymbol{\Phi}_1 + \boldsymbol{o}_{\kappa q}\boldsymbol{g}_\kappa^T & -\frac{\pi^2}{4\varphi_\kappa}\boldsymbol{\Phi}_1 \end{bmatrix},$$

$$\boldsymbol{\Phi}_{2\kappa q} \triangleq \begin{bmatrix} [\boldsymbol{A}_q\boldsymbol{X}_1 + *] - \frac{\pi^2}{4\phi_\kappa}\boldsymbol{\Phi}_1 & \frac{\pi^2}{4\phi_\kappa}\boldsymbol{\Phi}_1 - \boldsymbol{Y}_{\kappa q} \\ \frac{\pi^2}{4\phi_\kappa}\boldsymbol{\Phi}_1 - \boldsymbol{Y}_{\kappa q}^T & -\frac{\pi^2}{4\phi_\kappa}\boldsymbol{\Phi}_1 \end{bmatrix},$$

$$\boldsymbol{\Phi}_{3\kappa q} \triangleq \begin{bmatrix} -[\boldsymbol{X}_2\boldsymbol{\Theta} + *] & \boldsymbol{X}_2\boldsymbol{\Theta} & -\boldsymbol{Y}_{\kappa q} \\ \boldsymbol{\Theta}\boldsymbol{X}_2 & T_o^2\boldsymbol{X}_3 - 2\boldsymbol{X}_1 & \boldsymbol{Y}_{\kappa q} \\ -\boldsymbol{Y}_{\kappa q}^T & \boldsymbol{Y}_{\kappa q}^T & -\frac{\Delta\hat{x}_\kappa\boldsymbol{X}_3}{\Delta\bar{x}_\kappa} \end{bmatrix},$$

$$\boldsymbol{\Phi}_{4\kappa iq} \triangleq \begin{bmatrix} \boldsymbol{X}_1[\boldsymbol{A}_i-\boldsymbol{A}_q]^T & 0 \\ 0 & -\nu \boldsymbol{g}_\kappa \boldsymbol{o}_{\kappa q}^T \end{bmatrix},$$
$$\boldsymbol{\Phi}_{5\kappa q} \triangleq \begin{bmatrix} -\boldsymbol{X}_1\boldsymbol{A}_q^T & \boldsymbol{X}_1\boldsymbol{A}_q^T & \boldsymbol{Y}_{\kappa q} \\ \boldsymbol{Y}_{\kappa q}^T & -\boldsymbol{Y}_{\kappa q}^T & 0 \end{bmatrix}, \ \boldsymbol{\Phi}_{10} \triangleq \begin{bmatrix} \boldsymbol{X}_1 \\ 0 \end{bmatrix},$$
$$\boldsymbol{\Phi}_6 \triangleq \begin{bmatrix} -\boldsymbol{I} \\ \boldsymbol{I} \\ 0 \end{bmatrix}, \boldsymbol{\Phi}_8 \triangleq \begin{bmatrix} \boldsymbol{I} \\ 0 \end{bmatrix}, \boldsymbol{\Phi}_9 \triangleq \begin{bmatrix} \nu\boldsymbol{I} \\ 0 \end{bmatrix},$$
$$\boldsymbol{\Phi}_{7iq} \triangleq \begin{bmatrix} -\boldsymbol{X}_1[\boldsymbol{A}_i-\boldsymbol{A}_q]^T & \boldsymbol{X}_1[\boldsymbol{A}_i-\boldsymbol{A}_q]^T & 0 \\ 0 & 0 & 0 \end{bmatrix},$$

in which

$$\begin{aligned} &\Delta\bar{x}_\kappa \triangleq x_{\kappa+1}-x_\kappa, \ \kappa\in\mathfrak{M}, \\ &\varphi_\kappa \triangleq \max\{(x_\kappa^R-x_\kappa)^2,(x_{\kappa+1}-x_\kappa^L)^2\}, \ \kappa\in\mathfrak{M}, \\ &\phi_\kappa \triangleq \max\{(\hat{x}_\kappa^R-x_\kappa)^2,(x_{\kappa+1}-\hat{x}_\kappa^L)^2\}, \ \kappa\in\mathfrak{M}, \end{aligned} \tag{23}$$

then there is a spatiotemporal fuzzy-observer-based nonlinear compensator (10) and (14) exponentially stabilizing the nonlinear networked PDE system (1)-(4), where the gain parameters $\boldsymbol{k}_{\kappa q}$, $\boldsymbol{L}_{\kappa q}$, $\kappa\in\mathfrak{M}$, $q\in\mathfrak{S}$ are given by

$$\boldsymbol{k}_{\kappa q}^T=\boldsymbol{o}_{\kappa q}^T\boldsymbol{X}_1^{-1}, \ \boldsymbol{L}_{\kappa q}=\boldsymbol{Y}_{\kappa q}\boldsymbol{X}_1^{-1}, \ \kappa\in\mathfrak{M}, \ q\in\mathfrak{S}. \tag{24}$$

Proof: Given that the LMIs (22)-(24) are feasible for scalars $\nu>0$, $\sigma>0$, $\varepsilon>0$, matrices $0<\boldsymbol{X}_1\in\Re^{n\times n}$, $0<\boldsymbol{X}_2\in\Re^{n\times n}$, $0<\boldsymbol{X}_3\in\Re^{n\times n}$, $\boldsymbol{Y}_{\kappa q}\in\Re^{n\times n}$, and vectors $\boldsymbol{o}_{\kappa q}\in\Re^n$, $\kappa\in\mathfrak{M}$, $q\in\mathfrak{S}$. Set

$$\begin{aligned} &\boldsymbol{X}_1=\boldsymbol{P}_1^{-1}, \ \boldsymbol{X}_2=\boldsymbol{P}_2^{-1}, \ \boldsymbol{X}_3=\boldsymbol{P}_1^{-1}\boldsymbol{P}_3\boldsymbol{P}_1^{-1}, \\ &\boldsymbol{o}_{\kappa q}^T=\boldsymbol{k}_{\kappa q}^T\boldsymbol{X}_1, \ \boldsymbol{Y}_{\kappa q}=\boldsymbol{L}_{\kappa q}\boldsymbol{X}_1, \ \kappa\in\mathfrak{M}, \ q\in\mathfrak{S}. \end{aligned} \tag{25}$$

Via the property of the matrix $\boldsymbol{\Phi}_1$ and $\boldsymbol{P}_1>0$ and (25), the inequality (21) means

$$\boldsymbol{\Psi}_1 \triangleq [\boldsymbol{P}_1\boldsymbol{\Theta}+*]>0. \tag{26}$$

Similarly to the proof of Theorem 2 [49], in the light of integration by parts and Lemma 2 [49] with the inequality (26) and $[x_\kappa^L,x_\kappa^R]\subset(x_\kappa,x_{\kappa+1})$, $\kappa\in\mathfrak{M}$, along the solution to the system (15), for any $t\in[t_k,t_{k+1})$, $k\in\mathfrak{N}$, the following inequality is derived by taking derivative of $V_0(t)$ in (17):

$$\begin{aligned} \dot{V}_0(t) \le\ & \nu\sum_{\kappa=1}^m\int_{x_\kappa}^{x_{\kappa+1}}\hat{\boldsymbol{z}}_\kappa^T(x,t)\bar{\boldsymbol{\Psi}}_{1\kappa}(\boldsymbol{\zeta},\hat{\boldsymbol{\zeta}})\hat{\boldsymbol{z}}_\kappa(x,t)dx \\ &+2\nu\sum_{\kappa=1}^m\int_{x_\kappa}^{x_{\kappa+1}}\boldsymbol{z}^T(x,t)\boldsymbol{P}_1\Delta\boldsymbol{f}(\boldsymbol{z}(x,t))dx \\ &-2\nu\sum_{\kappa=1}^m\boldsymbol{z}_\kappa^T(t)\int_{x_\kappa}^{x_{\kappa+1}}\sum_{q=1}^s w_q(\hat{\boldsymbol{\zeta}})\boldsymbol{P}_1\boldsymbol{g}_\kappa\boldsymbol{k}_{\kappa q}^T\boldsymbol{e}(x,t)dx, \end{aligned} \tag{27}$$

where $\hat{\boldsymbol{z}}_\kappa(x,t)\triangleq[\boldsymbol{z}^T(x,t)\quad \boldsymbol{z}_\kappa^T(t)]^T$, $\boldsymbol{z}_\kappa(t)\triangleq\frac{1}{\Delta x_\kappa}\int_{x_\kappa^L}^{x_\kappa^R}\boldsymbol{z}(x,t)dx$ and

$$\begin{aligned} \bar{\boldsymbol{\Psi}}_{1\kappa}(\boldsymbol{\zeta},\hat{\boldsymbol{\zeta}}) \triangleq\ & \sum_{i,q=1}^s w_i(\boldsymbol{\zeta})w_q(\hat{\boldsymbol{\zeta}}) \\ &\times\begin{bmatrix} [\boldsymbol{P}_1\boldsymbol{A}_i+*]-\frac{\pi^2}{4\varphi_\kappa}\boldsymbol{\Psi}_1 & \frac{\pi^2}{4\varphi_\kappa}\boldsymbol{\Psi}_1+\boldsymbol{P}_1\boldsymbol{g}_\kappa\boldsymbol{k}_{\kappa q}^T \\ \frac{\pi^2}{4\varphi_\kappa}\boldsymbol{\Psi}_1+\boldsymbol{k}_{\kappa q}\boldsymbol{g}_\kappa^T\boldsymbol{P}_1 & -\frac{\pi^2}{4\varphi_\kappa}\boldsymbol{\Psi}_1 \end{bmatrix}, \end{aligned}$$

in which φ_κ, $\kappa\in\mathfrak{M}$ are defined by (23).

Define

$$\begin{aligned} \bar{\boldsymbol{e}}_\kappa(t,t_k) &\triangleq \int_0^L c_\kappa(x)\int_{t_k}^t\boldsymbol{e}_s(x,s)dsdx \\ &=\int_{x_\kappa}^{x_{\kappa+1}}\int_{t_k}^t\boldsymbol{e}_s(x,s)dsdx, \kappa\in\mathfrak{M}, k\in\mathfrak{N}, \end{aligned} \tag{28}$$

where $c_\kappa(x)$, $\kappa\in\mathfrak{M}$ are defined by (4). Similarly, applying Lemma 2 [49] with (26) and $[\hat{x}_\kappa^L,\hat{x}_\kappa^R]\subset(x_\kappa,x_{\kappa+1})$ again and using (28) and $\bigcup_{\kappa\in\mathfrak{M}}[x_\kappa,x_{\kappa+1}]=[0,L]$, along the solution to the system (13), for any $t\in[t_k,t_{k+1})$, $k\in\mathfrak{N}$, the following inequality is obtained by taking the derivative of $V_1(t)$ in (18)

$$\begin{aligned} \dot{V}_1(t) \le\ & \sum_{\kappa=1}^m\int_{x_\kappa}^{x_{\kappa+1}}\hat{\boldsymbol{e}}_\kappa^T(x,t)\bar{\boldsymbol{\Psi}}_{2\kappa}(\hat{\boldsymbol{\zeta}})\hat{\boldsymbol{e}}_\kappa(x,t)dx \\ &+2\sum_{\kappa=1}^m\int_{x_\kappa}^{x_{\kappa+1}}\boldsymbol{e}^T(x,t)\boldsymbol{P}_1\Delta\boldsymbol{f}(\boldsymbol{z}(x,t))dx \\ &+2\sum_{\kappa=1}^m\int_{x_\kappa}^{x_{\kappa+1}}\boldsymbol{e}^T(x,t)\boldsymbol{P}_1\sum_{i,q=1}^s w_i(\boldsymbol{\zeta})w_q(\hat{\boldsymbol{\zeta}}) \\ &\times[\boldsymbol{A}_i-\boldsymbol{A}_q]\boldsymbol{z}(x,t)dx \\ &+2\sum_{\kappa=1}^m\int_{x_\kappa}^{x_{\kappa+1}}\boldsymbol{e}^T(x,t)\boldsymbol{P}_1\sum_{q=1}^s w_q(\hat{\boldsymbol{\zeta}})\boldsymbol{L}_{\kappa q}dx\bar{\boldsymbol{e}}_\kappa(t,t_k), \end{aligned} \tag{29}$$

where $\hat{\boldsymbol{e}}_\kappa(x,t)\triangleq[\boldsymbol{e}^T(x,t)\quad \int_0^L c_\kappa(x)\boldsymbol{e}^T(x,t)dx]^T$,

$$\begin{aligned} \bar{\boldsymbol{\Psi}}_{2\kappa}(\hat{\boldsymbol{\zeta}}) \triangleq\ & \sum_{q=1}^s w_q(\hat{\boldsymbol{\zeta}}) \\ &\times\begin{bmatrix} [\boldsymbol{P}_1\boldsymbol{A}_q+*]-\frac{\pi^2}{4\phi_\kappa}\boldsymbol{\Psi}_1 & \frac{\pi^2}{4\phi_\kappa}\boldsymbol{\Psi}_1-\boldsymbol{P}_1\boldsymbol{L}_{\kappa q} \\ \frac{\pi^2}{4\phi_\kappa}\boldsymbol{\Psi}_1-\boldsymbol{L}_{\kappa q}^T\boldsymbol{P}_1 & -\frac{\pi^2}{4\phi_\kappa}\boldsymbol{\Psi}_1 \end{bmatrix}, \end{aligned}$$

and $\bar{\boldsymbol{e}}_\kappa(t,t_k)$, $\kappa\in\mathfrak{M}$, $k\in\mathfrak{N}$ are defined in (28).

Via integration by parts and $\bigcup_{\kappa\in\mathfrak{M}}[x_\kappa,x_{\kappa+1}]=[0,L]$, along the solution to the system (13), for any $t\in[t_k,t_{k+1})$, $k\in\mathfrak{N}$, the following expression is obtained by differentiating $V_2(t)$ defined in (19):

$$\begin{aligned} \dot{V}_2(t) =\ & -\sum_{\kappa=1}^m\int_{x_\kappa}^{x_{\kappa+1}}\boldsymbol{e}_{xx}^T(x,t)[\boldsymbol{P}_2\boldsymbol{\Theta}+*]\boldsymbol{e}_{xx}(x,t)dx \\ &-2\sum_{\kappa=1}^m\int_{x_\kappa}^{x_{\kappa+1}}\sum_{q=1}^s w_q(\hat{\boldsymbol{\zeta}})\boldsymbol{e}_{xx}^T(x,t)\boldsymbol{P}_2\boldsymbol{A}_q\boldsymbol{e}(x,t)dx \\ &+2\sum_{\kappa=1}^m\int_{x_\kappa}^{x_{\kappa+1}}\boldsymbol{e}_{xx}^T(x,t)\boldsymbol{P}_2\sum_{q=1}^s w_q(\hat{\boldsymbol{\zeta}})\boldsymbol{L}_{\kappa q}dx \\ &\times\int_0^L c_\kappa(x)\boldsymbol{e}(x,t)dx \\ &-2\sum_{\kappa=1}^m\int_{x_\kappa}^{x_{\kappa+1}}\boldsymbol{e}_{xx}^T(x,t)\boldsymbol{P}_2\Delta\boldsymbol{f}(\boldsymbol{z}(x,t))dx \\ &-2\sum_{\kappa=1}^m\int_{x_\kappa}^{x_{\kappa+1}}\boldsymbol{e}_{xx}^T(x,t)\boldsymbol{P}_2\sum_{i,q=1}^s w_i(\boldsymbol{\zeta})w_q(\hat{\boldsymbol{\zeta}}) \\ &\times[\boldsymbol{A}_i-\boldsymbol{A}_q]\boldsymbol{z}(x,t)dx \\ &-2\sum_{\kappa=1}^m\int_{x_\kappa}^{x_{\kappa+1}}\boldsymbol{e}_{xx}^T(x,t)\boldsymbol{P}_2\sum_{q=1}^s w_q(\hat{\boldsymbol{\zeta}})\boldsymbol{L}_{\kappa q}dx\bar{\boldsymbol{e}}_\kappa(t,t_k). \end{aligned} \tag{30}$$

The following inequality holds for $t \in [t_k, t_{k+1})$, $\boldsymbol{P}_3 > 0$ and $x \in [0, L]$ [39]

$$\int_{t_k}^{t} \boldsymbol{e}_s^T(x,s)\boldsymbol{P}_3\boldsymbol{e}_s(x,s)ds \geq \frac{1}{T_o}\int_{t_k}^{t} \boldsymbol{e}_s^T(x,s)ds\boldsymbol{P}_3\int_{t_k}^{t} \boldsymbol{e}_s(x,s)ds, \tag{31}$$

where the equality is fulfilled when $t = t_k$. Utilizing $\bigcup_{\kappa\in\mathfrak{M}}[x_\kappa, x_{\kappa+1}] = [0, L]$ and (31), the time derivative of $V_3(t)$ defined in (20) is obtained for any $t \in [t_k, t_{k+1})$, $k \in \mathfrak{N}$

$$\begin{aligned}\dot{V}_3(t) \leq\ & T_o^2\sum_{\kappa=1}^{m}\int_{x_\kappa}^{x_{\kappa+1}} \boldsymbol{e}_t^T(x,t)\boldsymbol{P}_3\boldsymbol{e}_t(x,t)dx \\ & -\sum_{\kappa=1}^{m}\int_{x_\kappa}^{x_{\kappa+1}}\int_{t_k}^{t} \boldsymbol{e}_s^T(x,s)ds\boldsymbol{P}_3\int_{t_k}^{t} \boldsymbol{e}_s(x,s)dsdx. \end{aligned}\tag{32}$$

Through the Jensen's inequality [53], the following expression is derived for any $[\hat{x}_\kappa^L, \hat{x}_\kappa^R] \subset (x_\kappa, x_{\kappa+1})$, $\kappa \in \mathfrak{M}$ and any $t \in [t_k, t_{k+1})$, $k \in \mathfrak{N}$

$$\begin{aligned}-\int_{x_\kappa}^{x_{\kappa+1}}\int_{t_k}^{t} \boldsymbol{e}_s^T(x,s)ds\boldsymbol{P}_3\int_{t_k}^{t} \boldsymbol{e}_s(x,s)dsdx \\ < -\Delta\hat{x}_\kappa\bar{\boldsymbol{e}}_\kappa^T(t,t_k)\boldsymbol{P}_3\bar{\boldsymbol{e}}_\kappa(t,t_k).\end{aligned}\tag{33}$$

Substitution of (33) into (32) gives

$$\begin{aligned}\dot{V}_3(t) <\ & T_o^2\sum_{\kappa=1}^{m}\int_{x_\kappa}^{x_{\kappa+1}} \boldsymbol{e}_t^T(x,t)\boldsymbol{P}_3\boldsymbol{e}_t(x,t)dx \\ & -\sum_{\kappa=1}^{m}\frac{\Delta\hat{x}_\kappa}{\Delta\bar{x}_\kappa}\int_{x_\kappa}^{x_{\kappa+1}} \bar{\boldsymbol{e}}_\kappa^T(t,t_k)\boldsymbol{P}_3\bar{\boldsymbol{e}}_\kappa(t,t_k)dx, \end{aligned}\tag{34}$$

where $\Delta\hat{x}_\kappa$ and $\Delta\bar{x}_\kappa$, $\kappa \in \mathfrak{M}$ are defined by (4) and (23).

Moreover, by $\bigcup_{\kappa\in\mathfrak{M}}[x_\kappa, x_{\kappa+1}] = [0, L]$, from (13) and (28), we have the following expression for any $t \geq 0$

$$\begin{aligned}0 =\ & 2\sum_{\kappa=1}^{m}\int_{x_\kappa}^{x_{\kappa+1}} \boldsymbol{e}_t^T(x,t)\boldsymbol{P}_1\boldsymbol{\Theta}\boldsymbol{e}_{xx}(x,t)dx \\ & + 2\sum_{\kappa=1}^{m}\int_{x_\kappa}^{x_{\kappa+1}}\sum_{q=1}^{s} w_q(\hat{\boldsymbol{\zeta}})\boldsymbol{e}_t^T(x,t)\boldsymbol{P}_1\boldsymbol{A}_q\boldsymbol{e}(x,t)dx \\ & - 2\sum_{\kappa=1}^{m}\int_{x_\kappa}^{x_{\kappa+1}} \boldsymbol{e}_t^T(x,t)\boldsymbol{P}_1\sum_{q=1}^{s} w_q(\hat{\boldsymbol{\zeta}})\boldsymbol{L}_{\kappa q}dx \\ & \times\int_0^L c_\kappa(x)\boldsymbol{e}(x,t)dx \\ & - 2\sum_{\kappa=1}^{m}\int_{x_\kappa}^{x_{\kappa+1}} \boldsymbol{e}_t^T(x,t)\boldsymbol{P}_1\boldsymbol{e}_t(x,t)dx \\ & + 2\sum_{\kappa=1}^{m}\int_{x_\kappa}^{x_{\kappa+1}} \boldsymbol{e}_t^T(x,t)\boldsymbol{P}_1\Delta\boldsymbol{f}(\boldsymbol{z}(x,t))dx \\ & + 2\sum_{\kappa=1}^{m}\int_{x_\kappa}^{x_{\kappa+1}} \boldsymbol{e}_t^T(x,t)\boldsymbol{P}_1\sum_{i,q=1}^{s} w_i(\boldsymbol{\zeta})w_q(\hat{\boldsymbol{\zeta}}) \\ & \times[\boldsymbol{A}_i - \boldsymbol{A}_q]\boldsymbol{z}(x,t)dx \\ & + 2\sum_{\kappa=1}^{m}\int_{x_\kappa}^{x_{\kappa+1}} \boldsymbol{e}_t^T(x,t)\boldsymbol{P}_1\sum_{q=1}^{s} w_q(\hat{\boldsymbol{\zeta}})\boldsymbol{L}_{\kappa q}dx\bar{\boldsymbol{e}}_\kappa(t,t_k). \end{aligned}\tag{35}$$

Under Assumption 2, the following inequality is fulfilled for any $\boldsymbol{z}(\cdot,t) \in \mathbb{D}$ and any constant $\sigma > 0$

$$\sigma\varepsilon\boldsymbol{z}^T(x,t)\boldsymbol{z}(x,t) - \sigma(\Delta\boldsymbol{f}(\boldsymbol{z}(x,t)))^T\Delta\boldsymbol{f}(\boldsymbol{z}(x,t)) > 0. \tag{36}$$

By using (27), (29), (30), and (34)-(36), and $\bigcup_{\kappa\in\mathfrak{M}}[x_\kappa, x_{\kappa+1}] = [0, L]$, for any $t \in [t_k, t_{k+1})$, $k \in \mathfrak{N}$, the time derivative of $V(t)$ defined by (16) is arranged as

$$\dot{V}(t) < \sum_{\kappa=1}^{m}\int_{x_\kappa}^{x_{\kappa+1}} \boldsymbol{\chi}_\kappa^T(x,t,t_k)\bar{\boldsymbol{\Psi}}_\kappa(\boldsymbol{\zeta},\hat{\boldsymbol{\zeta}})\boldsymbol{\chi}_\kappa(x,t,t_k)dx, \tag{37}$$

where $\boldsymbol{\chi}_\kappa(x,t,t_k) \triangleq [\hat{\boldsymbol{z}}_\kappa^T(x,t) \quad \boldsymbol{\xi}_\kappa^T(x,t,t_k) \quad (\Delta\boldsymbol{f}(\boldsymbol{z}(x,t)))^T]^T$, $\bar{\boldsymbol{\Psi}}_\kappa(\boldsymbol{\zeta},\hat{\boldsymbol{\zeta}}) \triangleq$

$$\begin{bmatrix} \nu\bar{\boldsymbol{\Psi}}_{1\kappa}(\boldsymbol{\zeta},\hat{\boldsymbol{\zeta}}) + \begin{bmatrix} \sigma\varepsilon\boldsymbol{I} & 0 \\ 0 & 0 \end{bmatrix} & \bar{\boldsymbol{\Psi}}_{4\kappa}(\hat{\boldsymbol{\zeta}}) & \bar{\boldsymbol{\Psi}}_7(\boldsymbol{\zeta},\hat{\boldsymbol{\zeta}}) & \bar{\boldsymbol{\Psi}}_9 \\ \bar{\boldsymbol{\Psi}}_{4\kappa}^T & \bar{\boldsymbol{\Psi}}_{2\kappa}(\hat{\boldsymbol{\zeta}}) & \bar{\boldsymbol{\Psi}}_{5\kappa}(\hat{\boldsymbol{\zeta}}) & \bar{\boldsymbol{\Psi}}_8 \\ \bar{\boldsymbol{\Psi}}_7^T(\boldsymbol{\zeta},\hat{\boldsymbol{\zeta}}) & \bar{\boldsymbol{\Psi}}_{5\kappa}^T(\hat{\boldsymbol{\zeta}}) & \bar{\boldsymbol{\Psi}}_{3\kappa}(\hat{\boldsymbol{\zeta}}) & \bar{\boldsymbol{\Psi}}_6 \\ \bar{\boldsymbol{\Psi}}_9^T & \bar{\boldsymbol{\Psi}}_8^T & \bar{\boldsymbol{\Psi}}_6^T & -\sigma\boldsymbol{I} \end{bmatrix},$$

with

$$\boldsymbol{\xi}_\kappa(x,t,t_k) \triangleq \begin{bmatrix}\hat{\boldsymbol{e}}_\kappa^T(x,t) & \boldsymbol{e}_{xx}^T(x,t) & \boldsymbol{e}_t^T(x,t) & \bar{\boldsymbol{e}}_\kappa^T(t,t_k)\end{bmatrix}^T,$$

$$\begin{aligned}\bar{\boldsymbol{\Psi}}_{3\kappa}(\hat{\boldsymbol{\zeta}}) \triangleq\ & \sum_{q=1}^{s} w_q(\hat{\boldsymbol{\zeta}}) \\ & \times\begin{bmatrix} -[\boldsymbol{P}_2\boldsymbol{\Theta} + *] & \boldsymbol{\Theta}\boldsymbol{P}_1 & -\boldsymbol{P}_2\boldsymbol{L}_{\kappa q} \\ \boldsymbol{P}_1\boldsymbol{\Theta} & T_o^2\boldsymbol{P}_3 - 2\boldsymbol{P}_1 & \boldsymbol{P}_1\boldsymbol{L}_{\kappa q} \\ -\boldsymbol{L}_{\kappa q}^T\boldsymbol{P}_2 & \boldsymbol{L}_{\kappa q}^T\boldsymbol{P}_1 & -\frac{\Delta\hat{x}_\kappa\boldsymbol{P}_3}{\Delta\bar{x}_\kappa} \end{bmatrix},\end{aligned}$$

$$\begin{aligned}\bar{\boldsymbol{\Psi}}_{4\kappa}(\boldsymbol{\zeta},\hat{\boldsymbol{\zeta}}) \triangleq\ & \sum_{i,q=1}^{s} w_i(\boldsymbol{\zeta})w_q(\hat{\boldsymbol{\zeta}}) \\ & \times\begin{bmatrix} [\boldsymbol{A}_i - \boldsymbol{A}_q]^T\boldsymbol{P}_1 & 0 \\ 0 & -\nu\boldsymbol{P}_1\boldsymbol{g}_\kappa\boldsymbol{k}_{\kappa q}^T \end{bmatrix},\end{aligned}$$

$$\bar{\boldsymbol{\Psi}}_{5\kappa}(\hat{\boldsymbol{\zeta}}) \triangleq \sum_{q=1}^{s} w_q(\hat{\boldsymbol{\zeta}})\begin{bmatrix} -\boldsymbol{A}_q^T\boldsymbol{P}_2 & \boldsymbol{A}_q^T\boldsymbol{P}_1 & \boldsymbol{P}_1\boldsymbol{L}_{\kappa q} \\ \boldsymbol{L}_{\kappa q}^T\boldsymbol{P}_2 & -\boldsymbol{L}_{\kappa q}^T\boldsymbol{P}_1 & 0 \end{bmatrix},$$

$$\bar{\boldsymbol{\Psi}}_6 \triangleq \begin{bmatrix} -\boldsymbol{P}_2 \\ \boldsymbol{P}_1 \\ 0 \end{bmatrix}, \bar{\boldsymbol{\Psi}}_8 \triangleq \begin{bmatrix} \boldsymbol{P}_1 \\ 0 \end{bmatrix}, \bar{\boldsymbol{\Psi}}_9 \triangleq \begin{bmatrix} \nu\boldsymbol{P}_1 \\ 0 \end{bmatrix},$$

$$\bar{\boldsymbol{\Psi}}_7(\boldsymbol{\zeta},\hat{\boldsymbol{\zeta}}) \triangleq \sum_{i,q=1}^{s} w_i(\boldsymbol{\zeta})w_q(\hat{\boldsymbol{\zeta}})\begin{bmatrix} -\boldsymbol{P}_2[\boldsymbol{A}_i - \boldsymbol{A}_q] & 0 \\ \boldsymbol{P}_1[\boldsymbol{A}_i - \boldsymbol{A}_q] & 0 \\ 0 & 0 \end{bmatrix}^T.$$

Pre- and post-multiplying $\bar{\boldsymbol{\Psi}}_\kappa(\boldsymbol{\zeta},\hat{\boldsymbol{\zeta}})$ with a block-diagonal matrix Block-diag$\{\boldsymbol{X}_1, \boldsymbol{X}_1, \boldsymbol{X}_1, \boldsymbol{X}_1, \boldsymbol{X}_2, \boldsymbol{X}_1, \boldsymbol{X}_1, \boldsymbol{I}\}$, we have

$$\begin{aligned}\bar{\boldsymbol{\Phi}}_\kappa(\boldsymbol{\zeta},\hat{\boldsymbol{\zeta}}) \triangleq\ & \sum_{i,q=1}^{s} w_i(\boldsymbol{\zeta})w_q(\hat{\boldsymbol{\zeta}}) \\ & \times\begin{bmatrix} \nu\boldsymbol{\Phi}_{1\kappa iq} + \begin{bmatrix} \sigma\varepsilon\boldsymbol{X}_1^2 & 0 \\ 0 & 0 \end{bmatrix} & \boldsymbol{\Phi}_{4\kappa iq} & \boldsymbol{\Phi}_{7iq} & \boldsymbol{\Phi}_9 \\ \boldsymbol{\Phi}_{4\kappa iq}^T & \boldsymbol{\Phi}_{2\kappa q} & \boldsymbol{\Phi}_{5\kappa q} & \boldsymbol{\Phi}_8 \\ \boldsymbol{\Phi}_{7iq}^T & \boldsymbol{\Phi}_{5\kappa q}^T & \boldsymbol{\Phi}_{3\kappa q} & \boldsymbol{\Phi}_6 \\ \boldsymbol{\Phi}_9^T & \boldsymbol{\Phi}_8^T & \boldsymbol{\Phi}_6^T & -\sigma\boldsymbol{I} \end{bmatrix}.\end{aligned}$$

By applying Schur complement and using (6) and (11), one can conclude that the following inequalities must be satisfied if the LMIs (22) are feasible:

$$\bar{\boldsymbol{\Phi}}_\kappa(\boldsymbol{\zeta},\hat{\boldsymbol{\zeta}}) < 0,\ \kappa \in \mathfrak{M}. \tag{38}$$

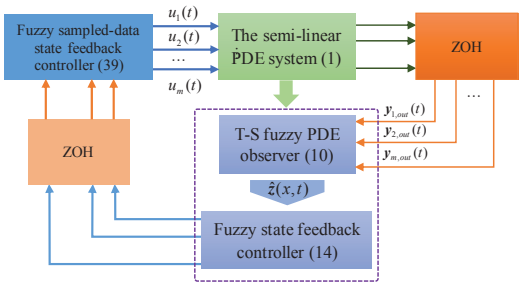

Fig. 6: A block diagram of the spatiotemporal fuzzy-observer-based nonlinear sampled-data compensator (39) with (10) and sampled-data measurement outputs

Via Theorem 3 in [54] and Theorem 1 in [55], we can conclude the exponential stability of the closed-loop augmented fuzzy PDE system (13) and (15) given that the inequalities (38) are fulfilled. From (25), we obtain (24). ■

Remark 4: Although only Dirichlet boundary conditions $z(0,t) = z(L,t) = 0$ are addressed in this article, the proposed design method is also applicable to the Neumann boundary conditions $z_x(x,t)|_{x=0} = z_x(x,t)|_{x=L} = 0$, the mixed Dirichlet-Neumann boundary conditions $z(0,t) = z_x(x,t)|_{x=L} = 0$, or the mixed Neumann-Dirichlet boundary conditions $z_x(x,t)|_{x=0} = z(L,t) = 0$. This is because $\mathcal{L}_n^2([0,L])$ is also separable for above boundary conditions. Moreover, the exponential stabilization ability of the fuzzy feedback compensator (10) can be enhanced by the inequality relaxation technique in Lemma 4 [39] or Lemma 3 [49].

B. Sampled-data control

Via the LMI-based design method in the above subsection, this subsection will discuss the design method development for the spatiotemporal fuzzy observer-based sampled-data feedback compensator that is used to model networked control, where control signals are transmitted from controller to actuators through the industrial internet. In this situation, the fuzzy state feedback controller (14) is fed into a ZOH (see Fig. 6) and the ZOH's output is revised as

$$u_\kappa(t) = \sum_{p=1}^{s} \int_{x_\kappa}^{x_{\kappa+1}} \bar{w}_p(\hat{\boldsymbol{\zeta}}(\bar{t}_k))\boldsymbol{k}_{\kappa p}^T \hat{\boldsymbol{z}}(x,\bar{t}_k)dx, \ \kappa \in \mathfrak{M}, \quad t \in [\bar{t}_k, \bar{t}_{k+1}), \ k \in \mathfrak{N}, \tag{39}$$

where $\bar{w}_p(\hat{\boldsymbol{\zeta}}(\bar{t}_k)) \triangleq \int_{x_\kappa}^{x_{\kappa+1}} w_p(\hat{\boldsymbol{\zeta}}(\hat{\boldsymbol{z}}(x,\bar{t}_k)))dx$, $p \in \mathfrak{S}$, the parameters $\boldsymbol{k}_{\kappa p} \in \Re^n$, $\kappa \in \mathfrak{M}$, $p \in \mathfrak{S}$ are to be determined, and the control signals $u_\kappa(t)$ are kept constant during the sampling period $[\bar{t}_k, \bar{t}_{k+1})$, $k \in \mathfrak{N}$ via the ZOH and are allowed to change only at the sampling moments $\bar{t}_k$, $k \in \mathfrak{N}$, in which $\bar{t}_{k+1} - \bar{t}_k \le T_u$, $k \in \mathfrak{N}$ and $T_u > 0$ is a constant given in advance. Moreover, the functions $\boldsymbol{g}_\kappa(x)$ are revised as follows

$$\boldsymbol{g}_\kappa(x) = \begin{cases} \frac{\boldsymbol{g}_\kappa}{\Delta\bar{x}_\kappa} & x \in (x_\kappa, x_{\kappa+1}), \\ 0 & \text{otherwise}, \end{cases} \quad \kappa \in \mathfrak{M}, \tag{40}$$

where $\Delta\bar{x}_\kappa$, $\kappa \in \mathfrak{M}$ are defined in (23).

By plugging the fuzzy controller (39) in the fuzzy PDE model (8) and considering $\boldsymbol{G}(x)$ in (40), and (12), we get the resulting closed-loop augmented fuzzy PDE system as the form (13) and the following PDE:

$$\begin{cases} \boldsymbol{z}_t(x,t) = \boldsymbol{\Theta}\boldsymbol{z}_{xx}(x,t) + \sum_{i=1}^{s} w_i(\boldsymbol{\zeta})\boldsymbol{A}_i\boldsymbol{z}(x,t) + \Delta\boldsymbol{f}(\boldsymbol{z}(x,t)) \\ \quad + \boldsymbol{g}_\kappa(x)\int_{x_\kappa}^{x_{\kappa+1}} \sum_{q=1}^{s} \bar{w}_q(\hat{\boldsymbol{\zeta}}(\bar{t}_k))\boldsymbol{k}_{\kappa q}^T \\ \quad \times[\boldsymbol{z}(x,\bar{t}_k) - \boldsymbol{e}(x,\bar{t}_k)]dx, \\ \quad x \in (0,L), \ t \in [\bar{t}_k, \bar{t}_{k+1}), \ k \in \mathfrak{N}, \ \kappa \in \mathfrak{M}, \\ \boldsymbol{z}(0,t) = \boldsymbol{z}(L,t) = 0, \ t \ge t_0, \\ \boldsymbol{z}(x,t_0) = \boldsymbol{z}_0(x), \ x \in [0,L]. \end{cases} \tag{41}$$

Definition 2 ([43]): The closed-loop fuzzy coupled PDEs (13) and (41) are exponentially stable in the norm $\|\cdot\|_{\mathcal{H}_n^1((0,L))}$ if for any $t > t_0$, one can find an integer $k \triangleq \lfloor tT_u^{-1} \rfloor$ ($k \triangleq \lfloor tT_u^{-1} \rfloor$ is a largest integer that is less than tT_u^{-1}) and four constants $\beta_3 > 0$, $\beta_4 > 0$, $\beta_5 > 0$ and $\beta_6 > 0$ satisfying

$$\begin{aligned} &\|\boldsymbol{z}(\cdot,t)\|_{\mathcal{H}_n^1((0,L))}^2 + \|\boldsymbol{e}(\cdot,t)\|_{\mathcal{H}_n^1((0,L))}^2 \\ &\quad \le \beta_4\|\boldsymbol{z}_0(\cdot)\|_{\mathcal{H}_n^1((0,L))}^2 \exp(-\beta_3 t) \\ &\quad + (\beta_5 + \beta_6 k\exp(\beta_3 T_u^{-1}))\|\boldsymbol{e}(\cdot)\|_{\mathcal{H}_n^1((0,L))}^2 \exp(-\beta_3 t) \\ &\quad + \beta_6\|\boldsymbol{e}(\cdot)\|_{\mathcal{H}_n^1((0,L))}^2 \exp(-\beta_3\bar{t}_k), \ t \in [\bar{t}_k, \bar{t}_{k+1}). \end{aligned}$$

Theorem 2: Consider the nonlinear PDE system (1), (3), (4), and (40) as well as the approximate fuzzy model (8) with Assumptions 1 and 2. Given an integer $m > 0$, some scalars $L > 0$, $T_o > 0$, $T_u > 0$, $\hat{x}_\kappa^L$, $\hat{x}_\kappa^R$, x_κ, $\kappa \in \mathfrak{M}$, and x_{m+1} ($0 = x_1 < x_2 < x_3 < \cdots < x_m < x_{m+1} = L$, and $[\hat{x}_\kappa^L, \hat{x}_\kappa^R] \subset (x_\kappa, x_{\kappa+1})$, $\kappa \in \mathfrak{M}$) and design parameters $\sigma > 0$ and $\varepsilon > 0$ (Assumption 2), if the LMI (21) and the following LMIs

$$\boldsymbol{\Phi}_4 \triangleq [\boldsymbol{\Theta}\boldsymbol{X}_4 + *] > 0, \tag{42}$$

$$\begin{bmatrix} \boldsymbol{\Phi}_{2\kappa q} & \boldsymbol{\Phi}_{5\kappa q} & \boldsymbol{\Phi}_8 \\ \boldsymbol{\Phi}_{5\kappa q}^T & \boldsymbol{\Phi}_{3\kappa q} & \boldsymbol{\Phi}_6 \\ \boldsymbol{\Phi}_8^T & \boldsymbol{\Phi}_6^T & -\sigma\boldsymbol{I} \end{bmatrix} < 0, \ \kappa \in \mathfrak{M}, \ q \in \mathfrak{S}, \tag{43}$$

$$\begin{bmatrix} \boldsymbol{\Upsilon}_{1\kappa ip} & \boldsymbol{\Upsilon}_{2\kappa ip} & \boldsymbol{\Phi}_8 & \boldsymbol{\Upsilon}_4 \\ \boldsymbol{\Upsilon}_{2\kappa ip}^T & \boldsymbol{\Upsilon}_{3\kappa p} & \boldsymbol{\Phi}_6 & 0 \\ \boldsymbol{\Phi}_8^T & \boldsymbol{\Phi}_6^T & -\sigma\boldsymbol{I} & 0 \\ \boldsymbol{\Upsilon}_4 & 0 & 0 & -\frac{\boldsymbol{I}}{2\sigma\varepsilon} \end{bmatrix} < 0, \ \kappa \in \mathfrak{M}, \ i,p \in \mathfrak{S}, \tag{44}$$

where

$$\boldsymbol{\Upsilon}_{1\kappa ip} \triangleq \begin{bmatrix} [\boldsymbol{A}_i\boldsymbol{X}_4 + *] - \frac{\pi^2}{(\Delta\bar{x}_\kappa)^2}\boldsymbol{\Phi}_4 & \frac{\pi^2}{(\Delta\bar{x}_\kappa)^2}\boldsymbol{\Phi}_4 + \boldsymbol{g}_\kappa\bar{\boldsymbol{o}}_{\kappa p}^T \\ \frac{\pi^2}{(\Delta\bar{x}_\kappa)^2}\boldsymbol{\Phi}_4 + \bar{\boldsymbol{o}}_{\kappa p}\boldsymbol{g}_\kappa^T & -\frac{\pi^2}{(\Delta\bar{x}_\kappa)^2}\boldsymbol{\Phi}_4 \end{bmatrix},$$

$$\boldsymbol{\Upsilon}_{3\kappa p} \triangleq \begin{bmatrix} -[\boldsymbol{X}_5\boldsymbol{\Theta} + *] & \boldsymbol{X}_5\boldsymbol{\Theta} & \boldsymbol{g}_\kappa\bar{\boldsymbol{o}}_{\kappa p}^T \\ \boldsymbol{\Theta}\boldsymbol{X}_5 & T_u^2\boldsymbol{X}_6 - 2\boldsymbol{X}_4 & -\boldsymbol{g}_\kappa\bar{\boldsymbol{o}}_{\kappa p}^T \\ \bar{\boldsymbol{o}}_{\kappa p}\boldsymbol{g}_\kappa^T & -\bar{\boldsymbol{o}}_{\kappa p}\boldsymbol{g}_\kappa^T & -\boldsymbol{X}_6 \end{bmatrix},$$

$$\boldsymbol{\Upsilon}_{2\kappa ip} \triangleq \begin{bmatrix} -\boldsymbol{X}_4\boldsymbol{A}_i^T & \boldsymbol{X}_4\boldsymbol{A}_i^T & -\boldsymbol{g}_\kappa\bar{\boldsymbol{o}}_{\kappa p}^T \\ -\bar{\boldsymbol{o}}_{\kappa p}\boldsymbol{g}_\kappa^T & \bar{\boldsymbol{o}}_{\kappa p}\boldsymbol{g}_\kappa^T & 0 \end{bmatrix}, \ \boldsymbol{\Upsilon}_4 \triangleq \begin{bmatrix} \boldsymbol{X}_4 \\ 0 \end{bmatrix},$$

are fulfilled for matrices $0 < \boldsymbol{X}_j \in \Re^{n\times n}$, $j \in \{1,2,3,4,5,6\}$, $\boldsymbol{Y}_{\kappa q} \in \Re^{n\times n}$ and vectors $\bar{\boldsymbol{o}}_{\kappa p} \in \Re^n$, $\kappa \in \mathfrak{M}$, $p,q \in \mathfrak{S}$, then one can construct a spatiotemporal fuzzy-observer-based nonlinear sampled-data compensator (10) and (39) exponentially stabilizing the networked PDE system (1), (3), (4), and (40) in the norm $\|\cdot\|_{\mathcal{H}_n^1((0,L))}$, where the gain parameters $\boldsymbol{k}_{\kappa p}$, $\boldsymbol{L}_{\kappa q}$, $\kappa \in \mathfrak{M}$, $p,q \in \mathfrak{S}$ are given by

$$\boldsymbol{k}_{\kappa p}^T = \bar{\boldsymbol{o}}_{\kappa p}^T\boldsymbol{X}_4^{-1}, \ \boldsymbol{L}_{\kappa q} = \boldsymbol{Y}_{\kappa q}\boldsymbol{X}_1^{-1}, \ \kappa \in \mathfrak{M}, \ p,q \in \mathfrak{S}. \tag{45}$$

Proof: This proof can be completed by replacing $V_0(t)$ in (17) by

$$\begin{aligned} V_0(t) = &\int_0^L \boldsymbol{z}^T(x,t)\boldsymbol{P}_4\boldsymbol{z}(x,t)dx \\ &+ \int_0^L \boldsymbol{z}_x^T(x,t)\boldsymbol{P}_5\boldsymbol{z}_x(x,t)dx \\ &+ T_u\int_0^L\int_{\bar{t}_k}^t (s-t+T_u)\boldsymbol{z}_s^T(x,s)\boldsymbol{P}_6\boldsymbol{z}_s(x,s)dsdx, \end{aligned}$$

where $\boldsymbol{P}_j > 0$, $j \in \{4,5,6\}$ are $n \times n$ Lyapunov matrices to be determined, and following proofs of Theorem 1, Theorem 1 [39], and Theorem 3.2 [43]. ■

Remark 5: It has been pointed out in [43] that as the spatiotemporal asynchronous sampling in control input and observation output (i.e., $[\hat{x}_\kappa^L, \hat{x}_\kappa^R] \subset (x_\kappa, x_{\kappa+1})$ and $\bar{t}_k \neq t_k$), Theorem 2 presents exponential stabilization via the spatiotemporal fuzzy-observer-based nonlinear sampled-data compensator (10) and (39) for the networked PDE system (1), (3), (4), and (40) in the sense of $\|\cdot\|_{\mathcal{H}_n^1((0,L))}$, which is different from the exponential stabilization in Theorem 1 via the spatiotemporal fuzzy-observer-based nonlinear continuous-time compensator (10) and (14) for the networked PDE system (1), (3), (4), and (2) in the norm $\|\cdot\|_2$.

IV. Simulation Study

For the sake of demonstrating the control performance of the spatiotemporal fuzzy compensators, we address feedback compensator of a multi-variable parabolic PDE system

$$\begin{cases} z_{1,t}(x,t) = z_{1,xx}(x,t) + 10z_1(x,t) - z_2(x,t) \\ \qquad\qquad -z_1^3(x,t) + \sum_{\kappa=1}^4 \bar{g}_\kappa(x)u_\kappa(t), \\ z_{2,t}(x,t) = z_{2,xx}(x,t) + 0.45z_1(x,t) - 0.1z_2(x,t) \\ z_i(0,t) = z_i(1,t) = 0,\ i \in \{1,2\}, \\ z_i(x,t_0) = z_{i,0}(x),\ i \in \{1,2\}, \end{cases} \tag{46}$$

where $z_1(x,t)$, $z_2(x,t)$ and $u_\kappa(t)$, $\kappa \in \{1,2,3,4\}$ are state variables and manipulated inputs, respectively, the distribution of these control inputs over the spatial domain $(0,1)$ is described by $\bar{g}_\kappa(x)$ of the form $\bar{g}_\kappa(x) = \begin{cases} \frac{1}{\Delta x_\kappa} & x \in [x_\kappa^L, x_\kappa^R] \\ 0 & \text{otherwise} \end{cases}$, with $x_1^L = 0.2$, $x_1^R = 0.3$, $x_2^L = 0.4$, $x_2^R = 0.5$, $x_3^L = 0.6$, $x_3^R = 0.7$, $x_4^L = 0.8$, and $x_4^R = 0.9$. When $z_1(x,t)$ is near zero, the nonlinear PDEs in (46) can be simplified as a linear PDE

$$\begin{cases} z_{1,t}(x,t) = z_{1,xx}(x,t) + 10z_1(x,t) - z_2(x,t) \\ \qquad\qquad +\sum_{\kappa=1}^4 \bar{g}_\kappa(x)u_\kappa(t), \\ z_{2,t}(x,t) = z_{2,xx}(x,t) + 0.45z_1(x,t) - 0.1z_2(x,t). \end{cases} \tag{47}$$

In the domain $\mathcal{D}(\bar{\boldsymbol{\mathcal{A}}}) \triangleq \{\bar{\boldsymbol{y}} \in \mathcal{H}_2^2((0,L)) : \bar{\boldsymbol{y}}(0) = \bar{\boldsymbol{y}}(L) = 0\}$, let define an operator $\bar{\boldsymbol{\mathcal{A}}}$ as $\boldsymbol{\mathcal{A}}\bar{\boldsymbol{y}}(x) \triangleq d^2\bar{\boldsymbol{y}}(x)/dx^2 + \boldsymbol{A}\bar{\boldsymbol{y}}(x)$, where $\bar{\boldsymbol{y}}(x) \triangleq [\bar{y}_1(x) \quad \bar{y}_2(x)]^T$ and $\boldsymbol{A} \triangleq \begin{bmatrix} 10 & -1 \\ 0.45 & -0.1 \end{bmatrix}$. The open-loop PDE of (47) is written as $\dot{\boldsymbol{z}}(t) = \bar{\boldsymbol{\mathcal{A}}}\boldsymbol{z}(t)$, where $\boldsymbol{z}(t) \triangleq \{\boldsymbol{z}(\cdot,t) : \boldsymbol{z}(x,t),\ x \in [0,L]\}$. By a simple but standard calculation, the first eigenvalue for $\bar{\boldsymbol{\mathcal{A}}}$ is 0.0856. Hence, the open-loop PDE of (47) is ***unstable***.

Set $t_0 = 0$ and the initial conditions $z_{i,0}(x)$, $i \in \{1,2\}$ in (46) to be $z_{1,0}(x) = x^3\cos(0.5\pi x)$ and $z_{2,0}(x) = 0$. The spatiotemporally asynchronous sampled-data observation outputs $\boldsymbol{y}_{\kappa,out}(t)$, $\kappa \in \{1,2,3,4\}$ are chosen of the form (3) with (4), where $T_o = 0.5$, $\hat{x}_1^L = 0.1$, $\hat{x}_1^R = 0.2$, $\hat{x}_2^L = 0.3$, $\hat{x}_2^R = 0.4$, $\hat{x}_3^L = 0.5$, $\hat{x}_3^R = 0.6$, $\hat{x}_4^L = 0.8$, and $\hat{x}_4^R = 0.9$. Fig. 7 provides evolution profiles of $z_i(x,t)$, $i \in \{1,2\}$ and trajectories of $|z_i(\cdot,t)|_2$, $i \in \{1,2\}$, $\|\boldsymbol{y}_{\kappa,out}(t)\|$, $\kappa \in \{1,2,3,4\}$ for the open-loop case. The simulation results in Fig. 7 show the instability of the system (46)'s steady profiles and $z_1(\cdot,t) \in (0,0.4)$, $t \geq 0$. The open set $\mathbb{D}$ is chosen as $\mathbb{D} = (-0.4, 0.4) \times (-\infty, \infty)$.

A. Approximate T-S fuzzy PDE model

When $z_1(x,t)$ is near ± 0.4, the nonlinear PDEs in (46) are simplified as

$$\begin{cases} z_{1,t}(x,t) = z_{1,xx}(x,t) + (10 - 3*0.39^2)z_1(x,t) \\ \qquad\qquad -z_2(x,t) + \sum_{\kappa=1}^4 \bar{g}_\kappa(x)u_\kappa(t), \\ z_{2,t}(x,t) = z_{2,xx}(x,t) + 0.45z_1(x,t) - 0.1z_2(x,t). \end{cases} \tag{48}$$

Note that (47) and (48) are now linear PDEs. We arrive at the following fuzzy PDE system based on the linear PDEs:

Model Rule 1:

IF z_1 is about zero, **THEN**

$$\begin{cases} \boldsymbol{z}_t(x,t) = \boldsymbol{z}_{xx}(x,t) + \boldsymbol{A}_1\boldsymbol{z}(x,t) + \boldsymbol{G}(x)\boldsymbol{u}(t), \\ \boldsymbol{z}(0,t) = \boldsymbol{z}(1,t) = 0,\ \boldsymbol{z}(x,t_0) = \boldsymbol{z}_0(x), \end{cases}$$

Model Rule 2:

IF z_1 is about ± 0.4 ($-0.4 < z_1(\cdot,t) < 0.4$), **THEN**

$$\begin{cases} \boldsymbol{z}_t(x,t) = \boldsymbol{z}_{xx}(x,t) + \boldsymbol{A}_2\boldsymbol{z}(x,t) + \boldsymbol{G}(x)\boldsymbol{u}(t), \\ \boldsymbol{z}(0,t) = \boldsymbol{z}(1,t) = 0,\ \boldsymbol{z}(x,t_0) = \boldsymbol{z}_0(x), \end{cases}$$

where $\boldsymbol{z}(x,t) \triangleq [z_1(x,t) \quad z_2(x,t)]^T$, $\boldsymbol{u}(t) \triangleq [u_1(t) \quad u_2(t) \quad u_3(t) \quad u_4(t)]^T$, $m = 4$, $\boldsymbol{g}_\kappa = [1 \quad 0]^T$, $\kappa \in \{1,2,3,4\}$, and

$$\boldsymbol{A}_1 = \begin{bmatrix} 10 & -1 \\ 0.45 & -0.1 \end{bmatrix} \text{ and } \boldsymbol{A}_2 = \begin{bmatrix} 10 - 3*0.39^2 & -1 \\ 0.45 & -0.1 \end{bmatrix}.$$

Under Assumption 1, the membership functions for Rules 1 and 2 can be chosen as $w_1(z_1) = \exp\left(-5z_1^2\right)$ and $w_2(z_1) = 1 - w_1(z_1)$, then the overall expression is written as

$$\begin{cases} \boldsymbol{z}_t(x,t) = \boldsymbol{z}_{xx}(x,t) + \sum_{i=1}^2 w_i(z_1)\boldsymbol{A}_i\boldsymbol{z}(x,t) \\ \qquad\qquad +\boldsymbol{G}(x)\boldsymbol{u}(t) + \Delta\boldsymbol{f}(\boldsymbol{z}(x,t)), \\ \boldsymbol{z}(0,t) = \boldsymbol{z}(1,t) = 0,\ \boldsymbol{z}(x,t_0) = \boldsymbol{z}_0(x), \end{cases} \tag{49}$$

where the error $\Delta\boldsymbol{f}(\boldsymbol{z})$ is presented as $\Delta\boldsymbol{f}(\boldsymbol{z}) \triangleq [-z_1^3 + 0.39^2 w_2(z_1)3z_1 \quad 0]^T$. It has been verified that the error $\Delta\boldsymbol{f}(\boldsymbol{z})$ satisfies $(\Delta\boldsymbol{f}(\boldsymbol{z}))^T\Delta\boldsymbol{f}(\boldsymbol{z}) - \varepsilon\boldsymbol{z}^T\boldsymbol{z} < 0$ for all $\boldsymbol{z} \in \mathbb{D}$ and $\varepsilon > 0.009$.

B. Continuous-time control

Set $\varepsilon = 0.1$, $x_1 = 0$, $x_2 = 0.3$, $x_3 = 0.5$, $x_4 = 0.7$, and $x_5 = 1$. Let $\sigma = 1$, $\nu = 1$, and $T_o = 0.5$. By solving LMIs (21) and (22) with $\boldsymbol{\Theta} = \boldsymbol{I}$ and using (24), the gain parameters $\boldsymbol{k}_{\kappa q}^T$ and $\boldsymbol{L}_{\kappa q}$, $\kappa \in \{1,2,3,4\}$, $q \in \{1,2\}$ for the

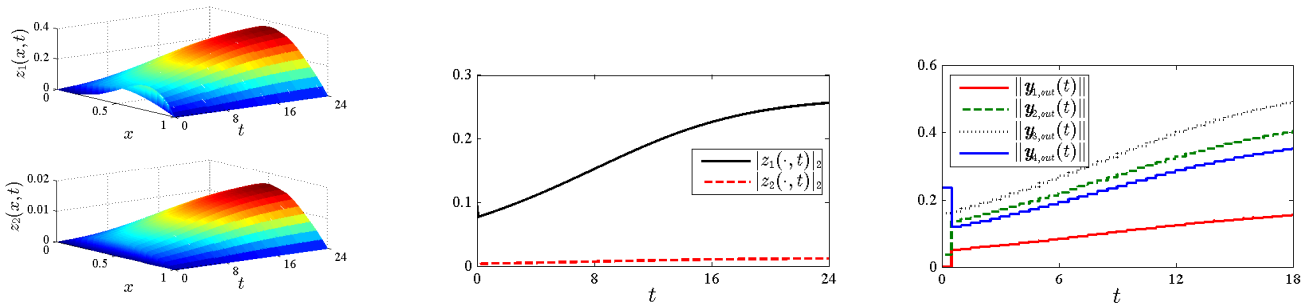

(a) (b) (c)

Fig. 7: Simulation results for the open-loop case: (a) evolution profiles of $z_i(x,t)$, $i \in \{1,2\}$, (b) trajectories of $|z_i(\cdot,t)|_2$, $i \in \{1,2\}$, and (c) trajectories of $\|\boldsymbol{y}_{\kappa,out}(t)\|$, $\kappa \in \{1,2,3,4\}$.

fuzzy observer-based continuous-time feedback compensator (10) and (14) are given as

$$\begin{bmatrix} \boldsymbol{k}_{11}^T \\ \boldsymbol{k}_{21}^T \\ \boldsymbol{k}_{31}^T \\ \boldsymbol{k}_{41}^T \end{bmatrix} = \begin{bmatrix} -0.1181 & 0.0246 \\ -0.1337 & 0.0113 \\ -0.1337 & 0.0113 \\ -0.1337 & 0.0113 \end{bmatrix},$$

$$\begin{bmatrix} \boldsymbol{k}_{12}^T \\ \boldsymbol{k}_{22}^T \\ \boldsymbol{k}_{32}^T \\ \boldsymbol{k}_{42}^T \end{bmatrix} = \begin{bmatrix} -0.0446 & 0.0144 \\ -0.1172 & 0.0087 \\ -0.1172 & 0.0087 \\ -0.1171 & 0.0087 \end{bmatrix},$$

$$\boldsymbol{L}_{11} = \boldsymbol{L}_{41} = \begin{bmatrix} 0.0230 & -0.0043 \\ 0.0007 & 0.0057 \end{bmatrix},$$

$$\boldsymbol{L}_{21} = \boldsymbol{L}_{31} = \begin{bmatrix} 0.0349 & -0.0064 \\ 0.0011 & 0.0082 \end{bmatrix},$$

$$\boldsymbol{L}_{12} = \begin{bmatrix} 0.0221 & -0.0043 \\ 0.0007 & 0.0057 \end{bmatrix},$$

$$\boldsymbol{L}_{22} = \boldsymbol{L}_{32} = \begin{bmatrix} 0.0335 & -0.0064 \\ 0.0011 & 0.0082 \end{bmatrix},$$

$$\boldsymbol{L}_{42} = \begin{bmatrix} 0.0221 & -0.0042 \\ 0.0007 & 0.0057 \end{bmatrix}.$$

By applying the fuzzy observer-based continuous-time feedback compensator (10) and (14) with the above gain parameters to the nonlinear system (46), Fig. 8 presents simulation results for the closed-loop case: evolution profiles of $z_i(x,t)$, $i \in \{1,2\}$, and trajectories of $|z_i(\cdot,t)|_2$, $i \in \{1,2\}$, $\boldsymbol{u}(t)$, and $\|\boldsymbol{y}_{\kappa,out}(t)\|$, $\kappa \in \{1,2,3,4\}$. The simulation results in Fig. 8 validate that the system (46) is stabilized by the fuzzy observer-based feedback controller (10) and (14).

C. Sampled-data control

Set $\varepsilon = 0.5$, $x_1 = 0$, $x_2 = 0.3$, $x_3 = 0.5$, $x_4 = 0.7$, and $x_5 = 1$. Let $\sigma = 1$, $T_o = 0.2$, and $T_u = 0.1$. By solving LMIs (21) and (42)-(44) with $\boldsymbol{\Theta} = \boldsymbol{I}$ and using (45), the gain parameters $\boldsymbol{k}_{\kappa p}^T$ and $\boldsymbol{L}_{\kappa q}$, $\kappa \in \{1,2,3,4\}$, $p,\ q \in \{1,2\}$ for the nonlinear observer-based sampled-data feedback compensator (10) and (39) are given as

$$\begin{bmatrix} \boldsymbol{k}_{11}^T \\ \boldsymbol{k}_{21}^T \\ \boldsymbol{k}_{31}^T \\ \boldsymbol{k}_{41}^T \end{bmatrix} = \begin{bmatrix} -0.4821 & 0.0632 \\ -0.2145 & 0.0289 \\ -0.2145 & 0.0289 \\ -0.4821 & 0.0632 \end{bmatrix},$$

$$\begin{bmatrix} \boldsymbol{k}_{12}^T \\ \boldsymbol{k}_{22}^T \\ \boldsymbol{k}_{32}^T \\ \boldsymbol{k}_{42}^T \end{bmatrix} = \begin{bmatrix} -0.4821 & 0.0632 \\ -0.2145 & 0.0289 \\ -0.2145 & 0.0289 \\ -0.4821 & 0.0632 \end{bmatrix},$$

$$\boldsymbol{L}_{11} = \boldsymbol{L}_{41} = \begin{bmatrix} 0.0694 & -0.0139 \\ 0.0019 & 0.0229 \end{bmatrix},$$

$$\boldsymbol{L}_{21} = \boldsymbol{L}_{31} = \begin{bmatrix} 0.1043 & -0.0208 \\ 0.0028 & 0.0328 \end{bmatrix},$$

$$\boldsymbol{L}_{12} = \boldsymbol{L}_{42} = \begin{bmatrix} 0.0665 & -0.0138 \\ 0.0019 & 0.0229 \end{bmatrix},$$

$$\boldsymbol{L}_{22} = \boldsymbol{L}_{32} = \begin{bmatrix} 0.0997 & -0.0206 \\ 0.0028 & 0.0328 \end{bmatrix}.$$

For the nonlinear systems (46) driven by the fuzzy observer-based sampled-data feedback compensator (10) and (39) with the above gain parameters, Fig. 9 presents the corresponding closed-loop simulation results: evolution profiles of $z_i(x,t)$, $i \in \{1,2\}$, and trajectories of $|z_i(\cdot,t)|_{\mathcal{H}_1^1((0,1))}$, $i \in \{1,2\}$, $\boldsymbol{u}(t)$, and $\|\boldsymbol{y}_{\kappa,out}(t)\|$, $\kappa \in \{1,2,3,4\}$. These simulation results support that the system (46) is stabilized by the fuzzy observer-based sampled-data feedback controller (10) and (39). Moreover, the simulation results in Figs. 8 and 9 reveal that the control performance for the continuous-time control is degraded for the case of sampled-data control.

D. Comparison study

To show the merit of the proposed fuzzy design method, this subsection provides a comparison study between the proposed fuzzy design method in Theorem 2 and a sampled-data proportional-derivative (PD) control law of the form:

$$u_\kappa(t) = \boldsymbol{k}_{P,\kappa}^T \boldsymbol{y}_{\kappa,out}(\bar{t}_k) + \boldsymbol{k}_{D,\kappa}^T \dot{\boldsymbol{y}}_{\kappa,out}(\bar{t}_k), \quad t \in [\bar{t}_k, \bar{t}_{k+1}), \kappa \in \{1,2,3,4\}, \tag{50}$$

where $\boldsymbol{k}_{P,\kappa} = [-0.6\ 0.02]^T$, $\boldsymbol{k}_{D,\kappa} = [0.1\ 0.1]^T$, and $\bar{t}_k = 0.1k$. Here we assume that the measurement outputs $\boldsymbol{y}_{\kappa,out}(\bar{t}_k)$,

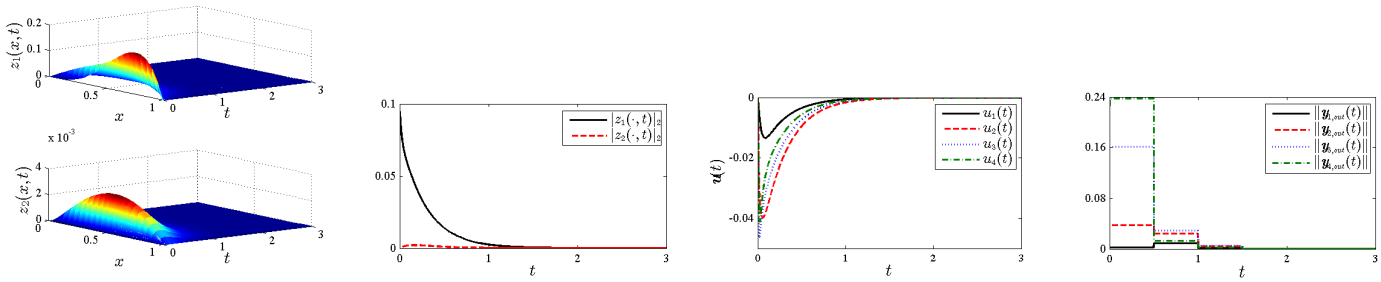

(a) (b) (c) (d)

Fig. 8: Simulation results for the closed-loop case: (a) evolution profiles of $z_i(x,t)$, $i \in \{1,2\}$, (b) trajectories of $|z_i(\cdot,t)|_2$, $i \in \{1,2\}$, and (c) trajectories of $\|\boldsymbol{y}_{\kappa,out}(t)\|$, $\kappa \in \{1,2,3,4\}$.

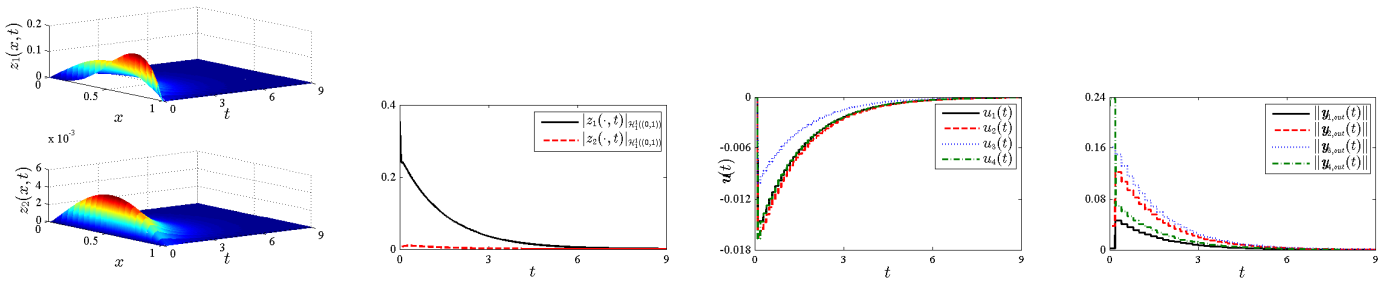

(a) (b) (c) (d)

Fig. 9: Simulation results for the closed-loop case: (a) evolution profiles of $z_i(x,t)$, $i \in \{1,2\}$, (b) trajectories of $|z_i(\cdot,t)|_{\mathcal{H}_1^1((0,1))}$, $i \in \{1,2\}$, and (c) trajectories of $\|\boldsymbol{y}_{\kappa,out}(t)\|$, $\kappa \in \{1,2,3,4\}$.

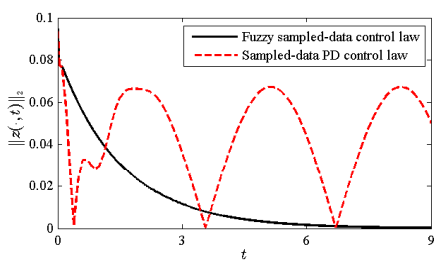

Fig. 10: Closed-loop trajectory of $\|\boldsymbol{z}(\cdot,t)\|_2$ driven by the sampled-data PD control law (50) and the spatiotemporal fuzzy sampled-data control law (39) with (10).

$\kappa \in \{1,2,3,4\}$ are exposed to the disturbance $0.1\sin(t)$. Fig. 10 shows the closed-loop trajectory of $\|\boldsymbol{z}(\cdot,t)\|_2$ driven by the sampled-data PD control law (50) and the spatiotemporal fuzzy sampled-data control law (39) with (10) and $T_u = T_o = 0.1$, whose gain parameters are chosen the same as the ones in above sampled-data control subsection. Simulation result in Fig. 10 reveals that compared to the PD control law, the proposed fuzzy control law performs a better robust performance to the measurement disturbances due to the existence of observer modular.

V. Conclusions

Based on the authors' previous works, from an estimation and fuzzy control perspective, this article has further dealt with nonlinear compensator design for stabilization of networked parabolic partial differential dynamic systems. An approximate T-S fuzzy PDE model with C^∞-smooth membership functions is proposed, which does not require the premise nonlinear dynamics. With the help of the approximate T-S fuzzy PDE model, spatiotemporal fuzzy-observer-based nonlinear continuous-time/sampled-data feedback compensators are constructed via the networked measurement outputs. Different from the exact T-S fuzzy PDE model, the approximate T-S fuzzy PDE model not only simplifies the T-S fuzzy model but also makes the suggested fuzzy compensator applicable to the nonlinear networked PDE systems with imprecise nonlinear dynamics. Moreover, the current work indicates that the observer-based feedback control technique can effectively surmount the design difficulty caused by the spatiotemporally asynchronous sampling in control and observation.

On the other hand, calculation consumption and performance optimization are very necessary and important for practical application. Different from the periodic sampled-data control methods, event-triggered control approaches transmit signals only when the user-designed triggering condition is violated, which greatly reduces the use of resources. Recently, adaptive dynamic programming (ADP) has appeared as an efficient method for optimal control of nonlinear systems to design approximate optimal control by using neural network-based function approximation. Although the spatiotemporal fuzzy control scheme of this article is proposed for sampled-data control of parabolic PDE systems on a simple 1-D space

domain, it is feasible to further deal with the spatiotemporal fuzzy optimal control design issue of nonlinear parabolic PDE systems on a general N-D space domain in the framework of event-triggered ADP. Moreover, it is also very interesting to discuss how to establish a general spatiotemporal fuzzy PDE model with continuous fuzzy membership functions and analyzing its approximation capability in a functional space.

REFERENCES

[1] W. Zhang, M. S. Branicky and S. M. Phillips, Stability of networked control systems, *IEEE Control Syst. Mag.*, vol. 21, no. 1, pp. 84–99, 2001.

[2] H. Ishii and B. A. Francis, *Limited Data Rate in Control Systems With Networks*, Berlin, Germany: Springer-Verlag, 2002.

[3] J. Qiu, H. Gao and S. X. Ding, Recent advances on fuzzy-model-based nonlinear networked control systems: A survey, *IEEE Trans. Ind. Electron.*, vol. 63, no. 2, pp. 1207–1217, 2016.

[4] R. A. Gupta and M.-Y. Chow, Networked control system: Overview and research trends, *IEEE Trans. Ind. Electron.*, vol. 57, no. 7, pp. 2527–2535, 2010.

[5] Y. Shi, J. Huang and B. Yu, Robust tracking control of networked control systems: Application to a networked DC motor, *IEEE Trans. Ind. Electron.*, vol. 60, no. 12, pp. 5864–5874, 2013.

[6] S. X. Ding, P. Zhang, S. Yin, and E. L. Ding, An integrated design framework of fault-tolerant wireless networked control systems for industrial automatic control applications, *IEEE Trans. Ind. Informat.*, vol. 9, no. 1, pp. 462–471, 2013.

[7] X.-M. Zhang, Q.-L. Han, X. Ge and L. Ding, Resilient control design based on a sampled-data model for a class of networked control systems under denial-of-service attacks, *IEEE Trans. Cybern.*, vol. 50, no. 8, pp. 3616-3626, 2020.

[8] T. Takagi and M. Sugeno, Fuzzy identification of systems and its applications to modeling and control, *IEEE Trans. Syst. Man, Cybern.*, vol. 15, no. 1, pp. 116–132, 1985.

[9] L.-X. Wang, *A Course in Fuzzy Systems and Control*, Prentice-Hall, Upper Saddle River, 1997.

[10] K. Tanaka and H. Wang, *Fuzzy Control Systems Design and Analysis: A Linear Matrix Inequality Approach*. New York: Wiley, 2001.

[11] G. Feng, *Analysis and Synthesis of Fuzzy Control Systems: A Model Based Approach*, Boca Raton, FL: CRC, 2010.

[12] H. Li, L. Wu, H.-K. Lam and Y. Gao, *Analysis and Synthesis for Interval Type-2 Fuzzy-Model-Based Systems*, New York: Springer, 2016.

[13] L. Wang and H.-K. Lam, H_∞ control for continuous-time Takagi-Sugeno fuzzy model by applying generalized Lyapunov function and introducing outer variables, *Automatica*, 2021, 125:109409.

[14] Y. Gao, F. Xiao, J. Liu and R. Wang, Distributed soft fault detection for interval Type-2 fuzzy-model-based stochastic systems with wireless sensor networks, *IEEE Trans. Ind. Inform.*, vol. 15, no. 1, pp. 334-347, 2019.

[15] H. Shen, F. Li, J. Cao, Z.-G. Wu and G. Lu, Fuzzy-model-based output feedback reliable control for network-based semi-Markov jump nonlinear systems subject to redundant channels, *IEEE Trans. Cybern.*, vol. 50, no. 11, pp. 4599-4609, 2020.

[16] Z. Lian, P. Shi and C. C. Lim, Dynamic hybrid-triggered-based fuzzy control for nonlinear networks under multiple cyberattacks, *IEEE Trans. Fuzzy Syst.*, vol. 30, no. 9, pp. 3940-3951, 2022.

[17] Z. Gu, C. K. Ahn, D. Yue and X. Xie, Event-triggered H_∞ filtering for T-S fuzzy-model-based nonlinear networked systems with multisensors against DoS attacks, *IEEE Trans. Cybern.*, vol. 52, no. 6, pp. 5311-5321, 2022.

[18] Z.-M. Li, X.-H. Chang and J. Xiong, Event-based fuzzy tracking control for nonlinear networked systems subject to dynamic quantization, *IEEE Trans. Fuzzy Syst.*, vol. 31, no. 3, pp. 941-954, 2023.

[19] H.-Y. Sun, H.-G. Han, J. Sun, H.-Y. Yang and J.-F. Qiao, Security control of sampled-data T-S fuzzy systems subject to cyberattacks and successive packet losses, *IEEE Trans. Fuzzy Syst.*, vol. 31, no. 4, pp. 1178-1188, 2023.

[20] Y. Wang, Y. Xia, C. K. Ahn, and Y. Zhu, Exponential stabilization of Takagi-Sugeno fuzzy systems with aperiodic sampling: An aperiodic adaptive event-triggered method, *IEEE Trans. Syst. Man Cybern. Syst.*, vol. 49, no. 2, pp. 444–454, 2019.

[21] C. Hua, S. Wu, and X. Guan, Stabilization of T-S fuzzy system with time delay under sampled-data control using a new looped-functional, *IEEE Trans. Fuzzy Syst.*, vol. 28, no. 2, pp. 400–407, 2020.

[22] Z. Zhang, S.-F. Su and Y. Niu, Dynamic event-triggered control for interval Type-2 fuzzy systems under fading channel, *IEEE Trans. Cybern.*, vol. 51, no. 11, pp. 5342-5351, 2021.

[23] W. Ji, J. Qiu, and H.-K. Lam, A new sampled-data output-feedback controller design of nonlinear systems via fuzzy affine models, *IEEE Trans. Cybern.*, vol. 52, no. 3, pp. 1681-1690, 2022.

[24] X.-L. Wang and G.-H. Yang, Robust filtering for fuzzy systems with bounded disturbances via premise-region-dependent event-triggered mechanisms, *IEEE Trans. Fuzzy Syst.*, vol. 30, no. 10, pp. 4093-4101, 2022.

[25] Z. You, H. Yan, H. Zhang, Y. Hu and S. Zhu, Aperiodic sampled-data-based control for T-S fuzzy systems: An improved fuzzy-dependent adaptive event-triggered mechanism, *IEEE Trans. Fuzzy Syst.*, vol. 31, no. 11, pp. 4085-4096, 2023.

[26] W. H. Ray, *Advanced Process Control*. New York: McGraw-Hill, 1981.

[27] P. D. Christofides, *Nonlinear and Robust Control of PDE Systems: Methods and Applications to Transport-Reaction Processes*. Boston, MA: Birkhauser, 2001.

[28] Y. Feng, Y. Wang, J.-W. Wang, and H.-X. Li, Backstepping-based distributed abnormality localization for linear parabolic distributed parameter systems, *Automatica*, vol. 135, Article No. 109930, 2022.

[29] W. He, S. S. Ge, B. V. How, et al, *Dynamics and Control of Mechanical Systems in Offshore Engineering*, London: Springer-Verlag, 2014.

[30] Y. Liu, Y. Fu, W. He, and Q. Hui, Modeling and observer-based vibration control of a flexible spacecraft with external disturbances, *IEEE Trans. Ind. Electron.*, vol. 66, no. 11, pp. 8648–8658, 2019.

[31] M.-B. Cheng, V. Radisavljevic, C.-C. Chang, et al., A sampled-data singularly perturbed boundary control for a heat conduction system with noncollocated observation, *IEEE Trans. Automat. Control*, vol. 54, no. 5, pp. 1305–1310, 2009.

[32] S. Ghantasala and N. H. EI-Farra, Active fault-tolerant control of sampled-data nonlinear distributed parameter systems, *Int. J. Robust Nonlinear Control*, vol. 22, no. 1, pp. 22–42, 2012.

[33] Z.-P. Wang and H.-N. Wu, Finite dimensional guaranteed cost sampled-data fuzzy control for a class of nonlinear distributed parameter systems, *Infor. Sci.*, vol. 327, pp. 21–39, 2016.

[34] H.-N. Wu and Z.-P. Wang, Observer-based H_∞ sampled-data fuzzy control for a class of nonlinear parabolic PDE systems, *IEEE Trans. Fuzzy Syst.*, vol. 26, no. 2, pp. 454–473, 2018.

[35] E. Fridman and A. Blighovsky, Robust sampled-data control of a class of semilinear parabolic systems, *Automatica*, vol. 48, no. 5, pp. 826-836, 2012.

[36] E. Fridman and N. Bar Am, Sampled-data distributed H_∞ control of transport reaction systems, *SIAM J. Control Optim.*, vol. 51, no. 2, pp. 1500-1527, 2013.

[37] A. Selivanov and E. Fridman, Sampled-data relay control of diffusion PDEs, *Automatica*, vol. 82, pp. 59–68, 2017.

[38] W.-H. Chen, S. Luo, and W.-X. Zheng, Sampled-data distributed H_∞ control of a class of 1-D parabolic systems under spatially point measurements, *J. Franklin Inst.*, vol. 354, no. 1, pp. 197–214, 2017.

[39] J.-W. Wang, S.-H. Tsai, H.-X. Li, and H.-K. Lam, Spatially piecewise fuzzy control design for sampled-data exponential stabilization of semilinear parabolic PDE systems, *IEEE Trans. Fuzzy Syst.*, vol. 26, no. 5, pp. 2967–2980, 2018.

[40] Z.-P. Wang, H.-N. Wu, and X.-H. Wang, Sampled-data fuzzy control with space-varying gains for nonlinear time-delay parabolic PDE systems, *Fuzzy Sets Syst.*, vol. 392, pp. 170–194, 2020.

[41] Q.-Q. Li, Z.-P. Wang, T. Huang, H.-N. Wu, H.-X. Li and J. Qiao, Fault-tolerant stochastic sampled-data fuzzy control for nonlinear delayed parabolic PDE systems, *IEEE Trans. Fuzzy Syst.*, vol. 31. no. 8, pp. 2679–2693, 2023.

[42] J.-W. Wang, Exponentially stabilizing observer-based feedback control of a sampled-data linear parabolic multiple-input-multiple-output PDE, *IEEE Trans. Syst. Man Cybern. Syst.*, vol. 51, no. 9, pp. 5742-5751, 2021.

[43] J.-W. Wang and J.-M. Wang, Spatiotemporally asynchronous sampled-data control of a linear parabolic PDE on a hypercube, *Int. J. Control*, vol. 95, no. 12, pp. 3326-3335, 2022.

[44] X. Song, Q. Zhang, S. Song and C. K. Ahn, Sampled-data-based event-triggered fuzzy control for PDE systems under cyberattacks, *IEEE Trans. Fuzzy Syst.*, vol. 30, no. 7, pp. 2693-2705, 2022.

[45] X. Song, Q. Zhang, Y. Zhang and S. Song, Fuzzy event-triggered control for PDE systems with pointwise measurements based on relaxed LyapunovCKrasovskii functionals, *IEEE Trans. Fuzzy Syst.*, vol. 30, no. 8, pp. 3074-3084, 2022.

[46] X. Song, R. Zhang, C. K. Ahn and S. Song, Adaptive event-triggered control of networked fuzzy PDE systems under hybrid cyber attacks, *IEEE Trans. Fuzzy Syst.*, vol. 30, no. 10, pp. 4211-4223, 2022.

[47] P. Gahinet, A. Nemirovskii, A. J. Laub, and M. Chilali, *LMI Control Toolbox for Use with Matlab, Natick*, MA: The Math.Works Inc., 1995.

[48] J.-W. Wang and H.-N. Wu, Exponential pointwise stabilization of semilinear parabolic distributed parameter systems via the Takagi-Sugeno fuzzy PDE model, *IEEE Trans. Fuzzy Syst.*, vol. 26, no. 1, pp. 155–173, 2018.

[49] J.-W. Wang and H.-X. Li, Static collocated piecewise fuzzy control design of quasi-linear parabolic PDE systems subject to periodic boundary conditions, *IEEE Trans. Fuzzy Syst.*, vol. 27, no. 7, pp. 1479-1492, 2019.

[50] B.-S. Chen and Y.-T. Chang, Fuzzy state-space modeling and robust observer-based control design for nonlinear partial differential systems, *IEEE Trans. Fuzzy Syst.*, vol. 17, no. 5, pp. 1025–1043, 2009.

[51] J. Robinson, *Infinite-Dimensional Dynamical Systems*. Cambridge, U. K.: Cambridge Univ. Press, 2001.

[52] J.-W. Wang, Y.-H. Wei, and P. Shi, Spatiotemporal adaptive fuzzy control for state profile tracking of nonlinear infinite-dimensional systems on a hypercube, *IEEE Trans. Fuzzy Syst.*, Available online, doi: 10.1109/T-FUZZ.2023.3307619, 2023.

[53] K. Gu, An integral inequality in the stability problem of time-delay systems, in *Proc. 39th IEEE Conf. Decision Control*, Sydney, Australia, 2000, pp. 2805–2810.

[54] J.-W. Wang and H.-N. Wu, Some extended Wirtinger's inequalities and distributed proportional-spatial integral control of distributed parameter systems with multi-time delays, *J. Franklin Inst.*, vol. 352, no. 10, pp. 4423–4445, 2015.

[55] J.-W. Wang, H.-X. Li, and H.-N. Wu, Fuzzy guaranteed cost sampled-data control of nonlinear systems coupled with a scalar reaction-diffusion process, *Fuzzy Sets Syst.*, vol. 302, pp. 121–142, 2016.

Jun-Wei Wang (Member, IEEE) received the B. S. degree in mathematics and applied mathematics and the M. S. degree in system theory both from Harbin Engineering University, Harbin, China, in 2007 and 2009, and the Ph. D. degree in control theory and control engineering from Beihang University, Beijing, China, in 2013, respectively.

He is currently working as an Associate Professor with the School of Intelligence Science and Technology, University of Science and Technology Beijing. His research interests include intelligent system modeling and control theory in infinite-dimensional space and multiple-robot coordination theory and its applications.

Yun Feng (Member, IEEE) received his B.E. degree in automation and M.S. degree in control theory and control engineering both from the Department of Automation, Wuhan University, Wuhan, China, in 2014 and 2017, respectively. He received the Ph.D. degree with the Department of Systems Engineering and Engineering Management, City University of Hong Kong, Hong Kong in 2020. From July to November 2019, he was a visiting student at the Institute for Automatic Control and Complex Systems (AKS), University of Duisburg-Essen, Germany.

He is currently an Associate Professor with the College of Electrical and Information Engineering, Hunan University, Changsha, China, and also with the National Engineering Research Center for Robot Visual Perception and Control Technology, Hunan University, Changsha, China. His research interests include distributed parameter systems, fault diagnosis, and soft robotics. He was selected for the Young Elite Scientists Sponsorship Program by the China Association for Science and Technology in 2023.

Stevan Dubljevic received the B.Sc. degree from Belgrade University, Belgrade, Serbia, in 1997, the M.Sc. degree from Texas A & M University, College Station, TX, USA, in 2001, and the Ph.D. degree from the Henry Samueli School of Engineering and Applied Science, University of California at Los Angeles, Los Angeles, CA, USA, in 2005.

He is currently an Associate Professor with the Department of Chemical and Materials Engineering, University of Alberta, Edmonton, AB, Canada. His research interests include systems engineering, with the emphasis on model predictive control of distributed parameter systems.

Hak-Keung Lam (Fellow, IEEE) received the B.Eng. (Hons.) degree in electronic engineering and the Ph.D. degree in electronic and information engineering from the Department of Electronic and Information Engineering, Hong Kong Polytechnic University, Hong Kong, in 1995 and 2000, respectively. During 2000-2005, he was a Postdoctoral Fellow and a Research Fellow with the Department of Electronic and Information Engineering, Hong Kong Polytechnic University. He joined as a Lecturer with Kings College London, London, U.K., in 2005 and is currently a Reader.

He has authored or coauthored three monographs: Stability Analysis of Fuzzy-Model-Based Control Systems (Springer, 2011), Polynomial Fuzzy Model Based Control Systems (Springer, 2016), and Analysis and Synthesis for Interval Type-2 Fuzzy-Model-Based Systems (Springer, 2016). His current research interests include intelligent control, computational intelligence, and machine learning. Dr. Lam was a Program Committee Member, an International Advisory Board Member, the Invited Session Chair, and the Publication Chair for various international conferences and a Reviewer for various books, international journals, and international conferences.

He was an Associate Editor for IEEE Transactions on Circuits and Systems II: Express Briefs, and is currently an Associate Editor for IEEE Transactions on Fuzzy Systems, IET Control Theory and Applications, International Journal of Fuzzy Systems, Neurocomputing, and Nonlinear Dynamics, and the Guest Editor for a number of international journals. He is currently on the Editorial Board of the Journal of Intelligent Learning Systems and Applications, Journal of Applied Mathematics, Mathematical Problems in Engineering, Modeling and Simulation in Engineering, Annual Review of Chaos Theory, Bifurcations and Dynamical System, The Open Cybernetics and Systemics Journal, Cogent Engineering, and International Journal of Sensors, Wireless Communications and Control. He was named as a highly cited Researcher. He is the Co-Editor of two edited volumes: Control of Chaotic Nonlinear Circuits (World Scientific, 2009) and Computational Intelligence and Its Applications (World Scientific, 2012).